consolidation low.

During the past year survey of this area, also ooze and ooze mixed with foraminiferal sand were collected from the foot to the base of the seamount, and samples consisting mostly of foraminiferal sand were recovered from the summit.

4 - 4 Chemical Composition of Rocks

From the basalt samples provided for microscopy, one sample which appeared least weathered was selected and analyzed chemically.

(1) Analytical methods

Analyzed elements and analytical methods are shown in Table 4-4-1, the analyzed elements and the limit of detection in Table 4-4-2. The samples were first washed and dried until constant weight and then they were prepared for analysis.

Table 4-4-1 Analytical methods and elements

Elements	Methods
SiO_2, TiO_2, Al_2O_3, Fe_2O_3, MnO, MgO, CaO, Na_2O, K_2O, P_2O_5,	ICP emission spectroscopy
FeO	Neutralization titration
CO_2	Combusion and infrated absorption spectroscopy (LECO)
H_2O^+, H_2O^-, LOI	Gravimetry
Rb, Sr, Ba, Zr, V, Nb, Y, La, Ce, Pr, Nd, Sm, Eu, Gd, Tb, Dy, Ho, Er, Tm, Yb, Lu	ICP mass spectroscopy

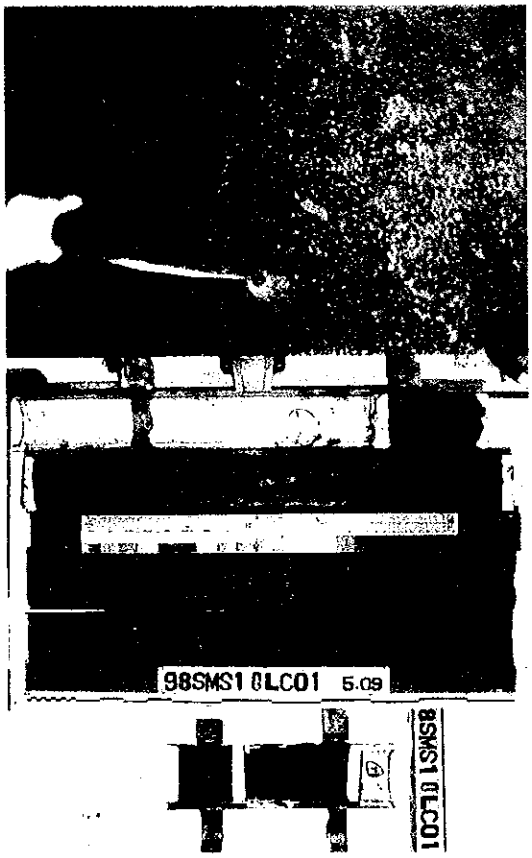

98SMS10LC01
Seafloor:Nodules overling seafloor.
Core:Ooze (320cm).nodule found on surface part.

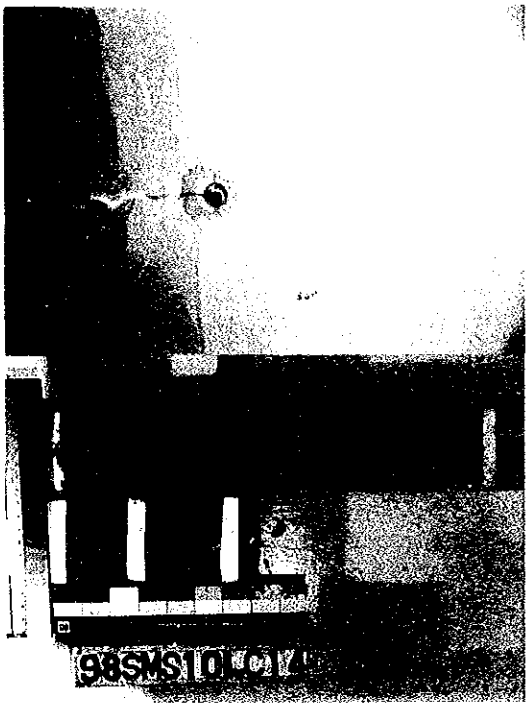

98SMS10LC14
Seafloor: Forminiferal sand and ripple marks.
Core: Forminiferal sand (78cm).

98SMS11LC11
Seefloor:Forminiferal sand covering botryoidal surface of crust.
Core: Not collected.

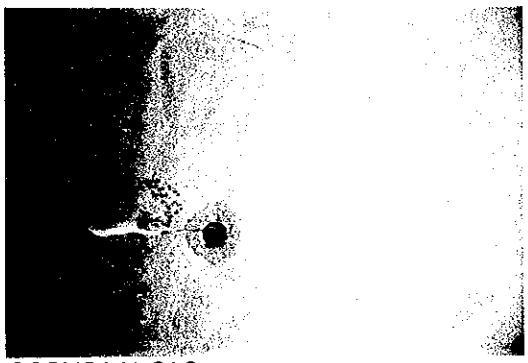

98SMS11LC12
Seafloor: Forminiferal sand with ripple mark covering botryoidal surface of crust.
Core: Not collected.

Fig. 4-3-2(1) Photographs of seafloor and unconsolidated sediments

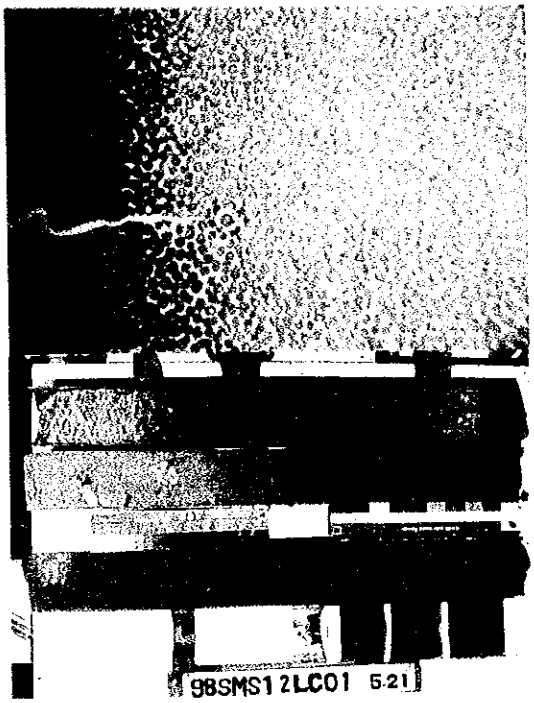

98SMS12LC01
Seafloor: Nodule covering ooze.
Core: Radish Brown ooze(325cm), pipe-like trace developed.

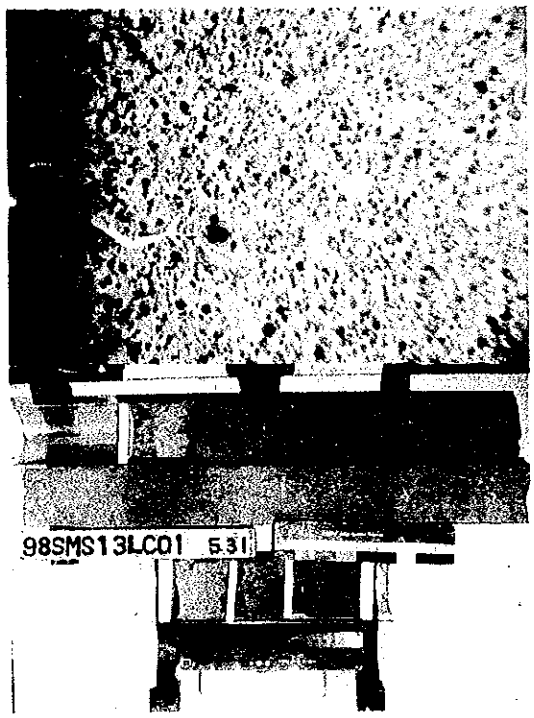

98SMS13LC01
Seafloor:Nodules scattering on calcareous clay surface.
Core: calcareous clay (215cm),including micro-nodule in the whole.

Fig. 4-3-2(2) Photographs of seafloor and unconsolidated sediments

Table 4-4-2 **the analysed componentw and the limit of detection**

35 Elements	14 major elements	SiO_2, TiO_2, Al_2O_3, Fe_2O_3, FeO, MnO, MgO, CaO, Na_2O, K_2O, P_2O_5, CO_2, H_2O^+, H_2O^-, LOI limit of detection; 0. 01%
	21 minor elements	Sr, Ba, Zr, V, Y limit of detection; 1ppm Rb, Nb, La, Ce, Pr, Nd, Sm, Eu, Gd, Tb, Dy, Ho, Er, Tm, Yb, Lu limit of detection; 0. 1ppm

(2) Results of analysis

The results of chemical analysis are laid out in Table 4-4-3 (1), (2). Various analytical diagrams were prepared on the basis of the chemical analysis. The following is the results.

1) Norm calculation

The results of norm calculation are laid out in Table 4-4-4 and norm diagram is shown in figure 4-4-1.

Basalt from MS10 area is in the olivine tholeiite group, and those from other three areas are in the tholeiite group.

Basalt from MS10 and MS11 areas have high normative apatite values. This is believed to be caused by apatite filling the fractures and voids in the rock. Also basalt from MS10 and MS11 areas show high normative hematite values and this is believed to be the effect of weathering.

2) AFM diagram

AFM diagram is shown in Figure 4-4-2.

Basalt samples from MS10 and MS11 areas are rich in FeO^* and poor in MgO and are plotted in the tholeiite position. Basalt samples from MS12 and MS13 areas is somewhat poor in FeO^* and are plotted in calk-alkaline basalt position.

3) Spider diagram of MORB normalized incompatible elements

Spider diagrams of normalized HFS elements and LIL elements of each sample are shown in Figure 4-4-3. Mile ORB values of Benvins et al., (1984) were used for normalization.

Table 4-4-3(1) Results of chemical analysis for rocks (main elements)

Sample No.	SiO2 %	TiO2 %	Al2O3 %	Fe2O3 %	FeO %	MnO %	MgO %	CaO %	Na2O %	K2O %	P2O5 %	H2O+ %	H2O- %	CO2 %	LOI %	TOTAL %	FeO*	Mg#
98SMS10AD05CA01	34.19	1.41	12.74	10.04	<0.1	0.29	2.04	16.08	2.95	1.49	8.26	3.73	2.69	1.49	8.54	98.04	9.08	0.183
98SMS11AD09CA01	35.67	1.79	13.63	12.4	<0.1	0.21	1.04	14.97	2.71	1.65	7.27	3.06	2.42	1.03	7.07	98.41	11.21	0.085
98SMS12AD07CA01	45.58	1.88	15.16	7.6	1.40	0.15	4.5	9.09	3.4	1.15	1.81	5.15	1.97	0.26	7.7	99.43	8.24	0.353
98SMS13AD03CA01	47.11	2.56	15.69	7.91	0.70	0.05	2.73	5.25	3.57	1.77	1.12	6.87	2.51	0.13	10.43	98.92	7.82	0.259

Table 4-4-3(2) Results of chemical analysis for rocks (rare elements)

Sample No.	V ppm	Rb ppm	Sr ppm	Y ppm	Zr ppm	Nb ppm	Ba ppm	La ppm	Ce ppm	Pr ppm	Nd ppm	Sm ppm	Eu ppm	Gd ppm	Tb ppm	Dy ppm	Ho ppm	Er ppm	Tm ppm	Yb ppm	Lu ppm
98SMS10AD05CA01	138	25	543	265	92	17	197	111	28	12.60	57.0	11.0	3.1	13.0	2.3	16.0	4.0	13.0	1.93	12.0	2.1
98SMS11AD09CA01	197	40	416	329	44	25	168	209	43	35.20	157.0	28.0	7.51	34.0	5.3	33.0	7.5	21.0	2.85	17.0	2.73
98SMS12AD07CA01	131	26	378	34	111	22	162	24	37	5.05	23.0	5.4	1.89	5.5	0.9	4.9	0.9	2.5	0.33	1.9	0.31
98SMS13AD03CA01	80	24	530	26	381	25	342	27	72	8.06	38.0	9.2	3.09	7.9	1.1	5.4	0.9	2.1	0.22	1.2	0.17

Table 4-4-4 Results of normative calculation

Sample No.	Q	C	or	ab	an	wo-di	en-di	fs-di	en-hy	fs-hy	fo-ol	cs	mt	hm	il	tn	pf	ru	ap	cc
98SMS10AD05CA01	1.20	0.26	8.81	24.96	16.40	2.13	1.84		5.08		2.27			10.04	0.72	2.48	0.03	1.03	19.14	3.39
98SMS11AD09CA01	3.31		9.75	22.93	20.15	0.58	0.50		2.59					12.40	0.55	0.08		1.47	16.84	2.34
98SMS12AD07CA01	2.96		6.80	28.77	22.71	3.50	3.02		8.18					7.60	3.28	0.38			4.19	0.59
98SMS13AD03CA01	7.77	1.34	10.46	30.21	17.91				6.80					7.91	1.58			1.73	2.59	0.30

Q: Quartz
C: Corundum
or: Orthoclase
ab: Albite
an: Anorthite

wo-di: Wollastonite-diopside
en-di: Enstatite-diopside
fs-di: Ferroselite-diopside
en-hy: Enstatite-hypersthene
fs-hy: Ferroselite-hypersthene

fo-ol: Fayalite
cs: Cyclosilicate calcium
mt: magnetite
hm: Hematite
il: Ilmenite

tn: Titanite
pf: Perovskite
ru: Rutile
ap: Apatite
cc: Calcite

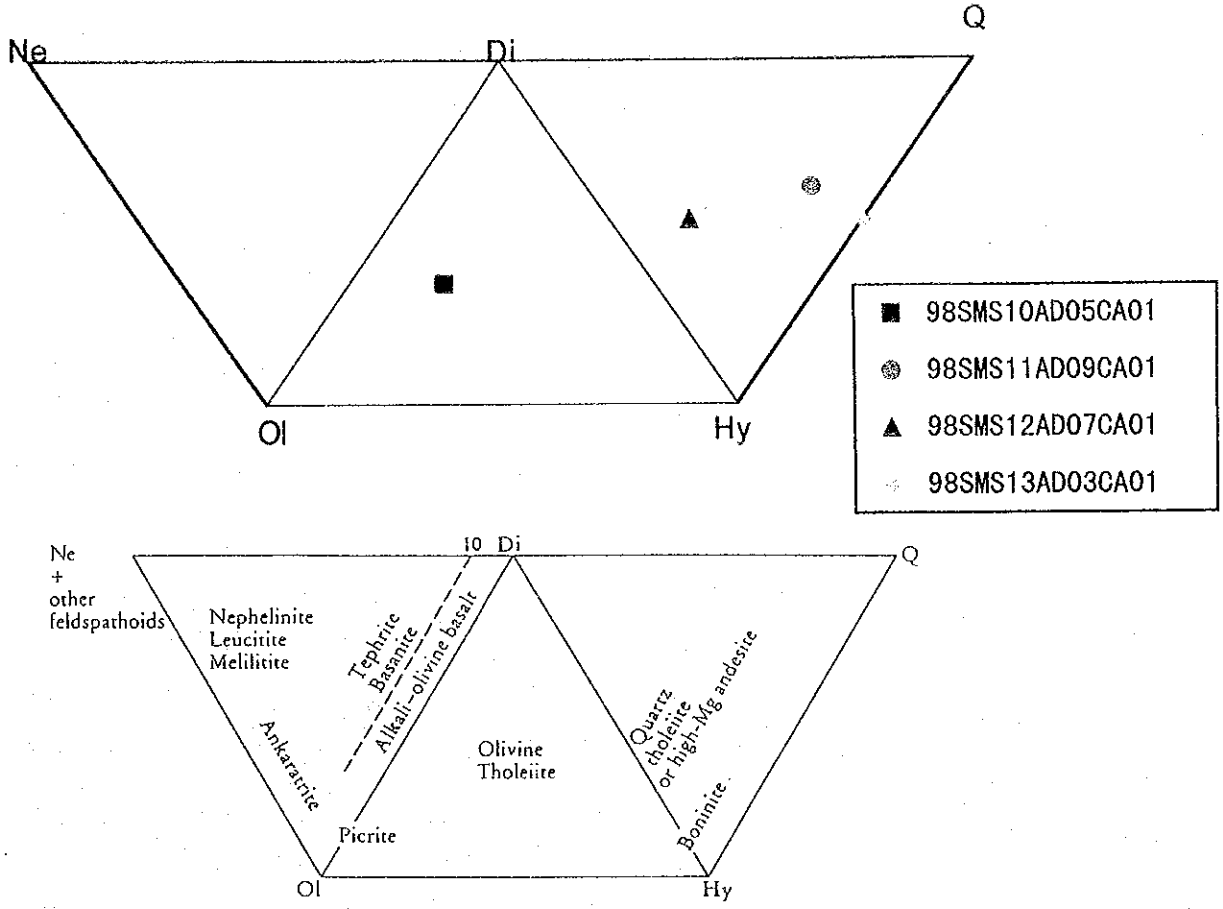

The classification of basalts and related basic and ultrabasic magmatic rocks according to their CIPW normative composition expressed as Ne–Ol–Di, Ol–Di–Hy or Di–Hy–Q (after Thompson, 1984).

Fig4-4-1 Normative composition diagram

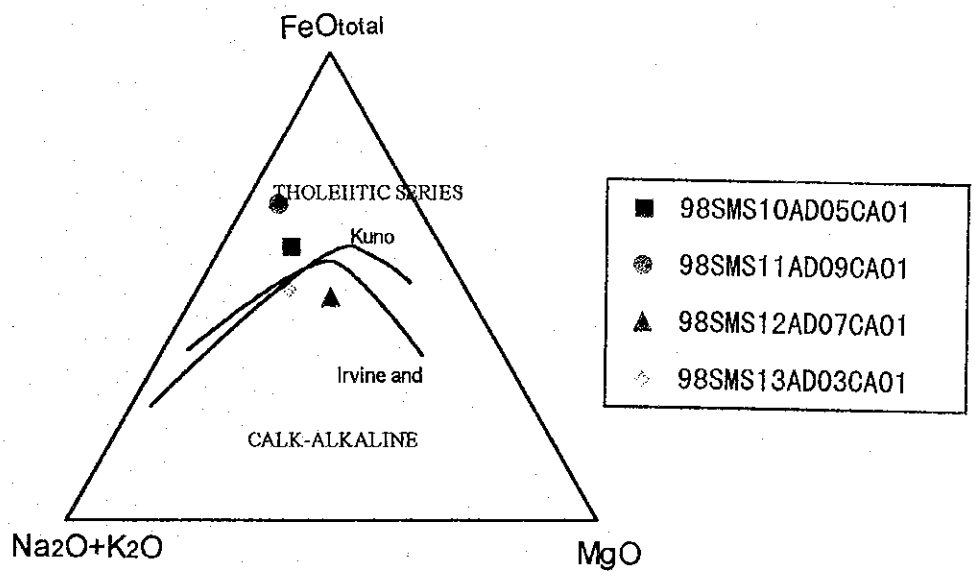

Fig4-4-2 AFM diagram

Basalt samples from MS10 and MS11 areas have LIL peaks at Rb, and show pattern of high P,Y for HFS elements and low Zr.

Basalt samples from MS13 area show pattern of increase from Sr to Ba for LIL elements and decrease from Nb to Y for HFS elements.

The sample from MS12 area has peaks at Rb for LIL elements and P for HFS elements and generally decrease from Nb to Y.

In all samples the effect of apatite which fills the voids and cracks are seen in their patterns. Thus these diagrams cannot be simply overlaid on the HFS and LIL element spider diagrams of typical basalts, but all diagrams have similar characteristics to those of oceanic island tholeiite and oceanic island basalt.

4) Spider diagrams of chondrite normalized rare earth elements

Spider diagrams of chondrite normalized REE of each sample are shown in Figure 4-4-4. Chondrite values of Wakita et al., (1971) were used for normalization.

Basalt samples from MS10 and MS11 areas have patterns with notable negative peak at Ce, and the inclination of the patterns is gentle from Eu. Basalt samples from MS12 and MS13 areas have linear patterns with steep inclination.

Comparing these patterns with REE spider diagrams of basalt in tectonic environment , the basalt samples from MS12 and MS13 areas show both values and patterns similar to those of oceanic island alkali basalt (OIA). Those from MS10 and MS11 areas have many differences such as the inclination of the patterns, notable negative peak at Ce, but as a whole the patterns are close to those of oceanic island alkali basalt.

5) Characteristics and division

Division of basalt using various diagrams is as follows.

① TiO_2-MnO-P_2O_5 diagram (Fig. 4-4-5)

All samples are plotted in the P_2O_5 -rich oceanic island alkali basalt area.

② Ti-V diagram (Fig. 4-4-6)

All samples are plotted in a position somewhat lower in V than oceanic island alkali basalt area.

③ Zn-Nb-Y diagram (Fig. 4-4-7)

The MS12 basalt samples are plotted in the E-type MORB area. The other three samples are plotted in positions off the area; namely those from MS10 and MS11 areas are in Y-rich position while those from

MS13 area in Y-poor, Nb-rich position.

The division considering; norm calculation, AFM diagram, HFS and LIL elements spider diagram, REE spider diagram, and various diagrams; is shown in Table 4-4-5. The division of basalt from each locality is considered from the above results.

MS10 area (98SMS10AD05CA01)

The basalt collected from MS13 area is inferred to be oceanic island alkali basalt from the study of; HFS, LIL element spider diagram, REE spider diagram, and $Ti0_2$-MnO-P_2 O_5 diagram. P, Zr, Y, Ce values are noted to differ from typical oceanic island alkali basalt, but this is considered to be caused by replacement of elements due to accretion of apatite and alteration because white argillaceous veinlets are developed in the samples and alteration is strong. Also large amounts of normative diopside and hypersthene were calculated due to replacement of elements, and thus this sample was classified as tholeiite by norm values and AMF diagram.

MS11 area (98SMS11AD09CA01)

This basalt is also inferred to be oceanic island alkali basalt. This sample shows trends very similar to MS10 basalt in all diagrams, and chemical nature is also close. The weathering noted by thin section microscopy is weak, but the results of chemical analysis indicate strong alteration as MS10 basalt.

MS12 area (98SMS12AD07CA01)

Basalt from MS12 area show characteristics of both alkali basalt and tholeiite after due consideration of the effect of weathering and alteration. However, it is believed to be appropriate to classify this basalt as oceanic island alkali basalt because; there is a clear difference from tholeiite in the values and pattern of the spider diagram of the HFS elements and LIL elements, and the spider diagram pattern of REE which is not easily affected by weathering is similar to that of oceanic island alkali basalt. This sample is also appears to be weakly altered, but the chemical results indicate weathering similar to the basalt from MS10 area.

MS13 area (98SMS13AD03CA01)

The basalt collected from MS13 area is inferred to be oceanic alkali basalt from the study of; HFS, LIL element spider diagram, REE spider diagram, and various diagrams. Also the high $NaO+K_2O$ content is in agreement with the above. The high H_2 O^+ value is due to the argillization confirmed by microscopy.

Basalt samples were collected from seamounts in MS01~MS09 with the exception of MS07 during the surveys in 1996 and this year. These samples are all classified as oceanic island alkali basalt as a result of chemical analysis. This is harmonious with the theory that the oceanic islands and seamounts of the Marshall Islands were

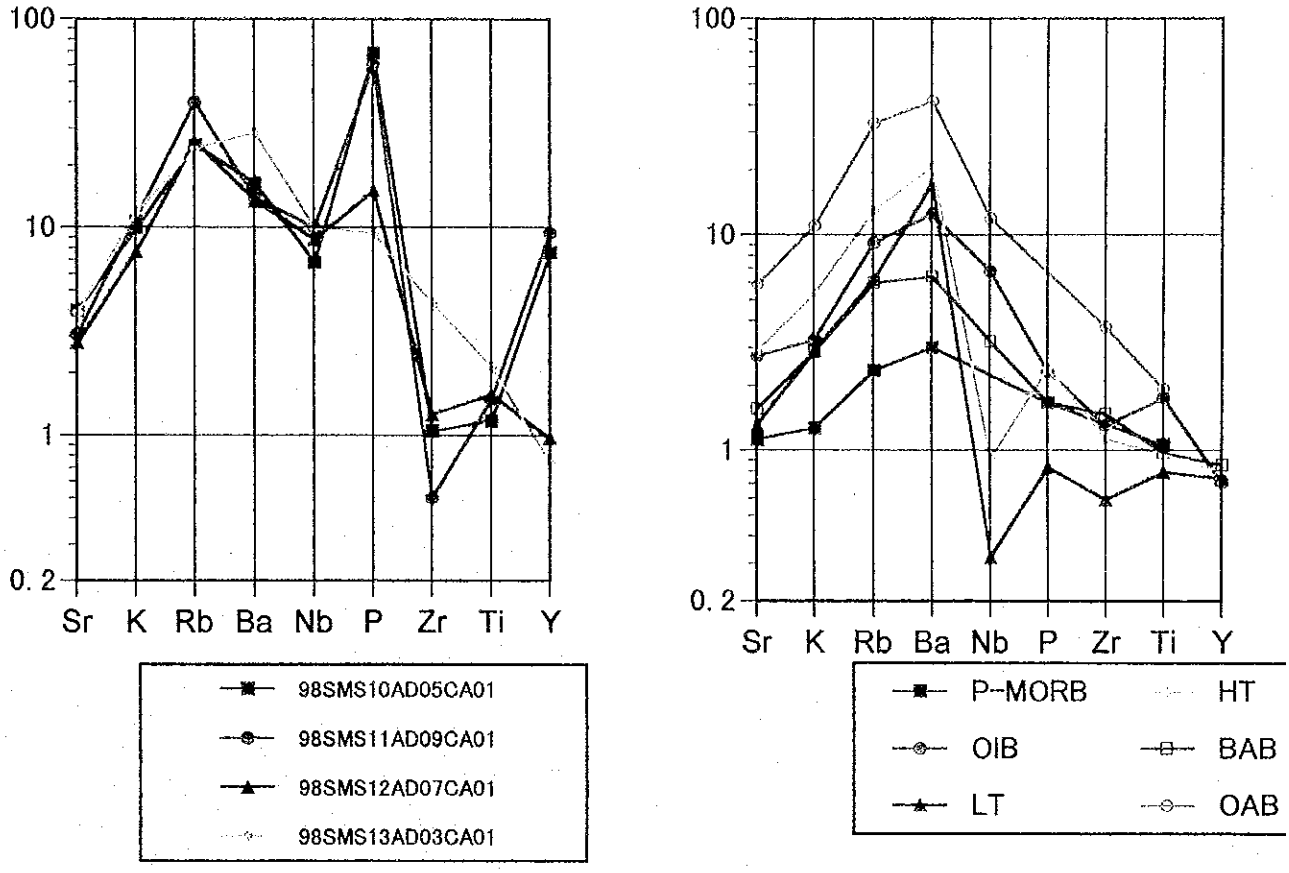

Fig. 4-4-3 Spidergram of incompatible elements

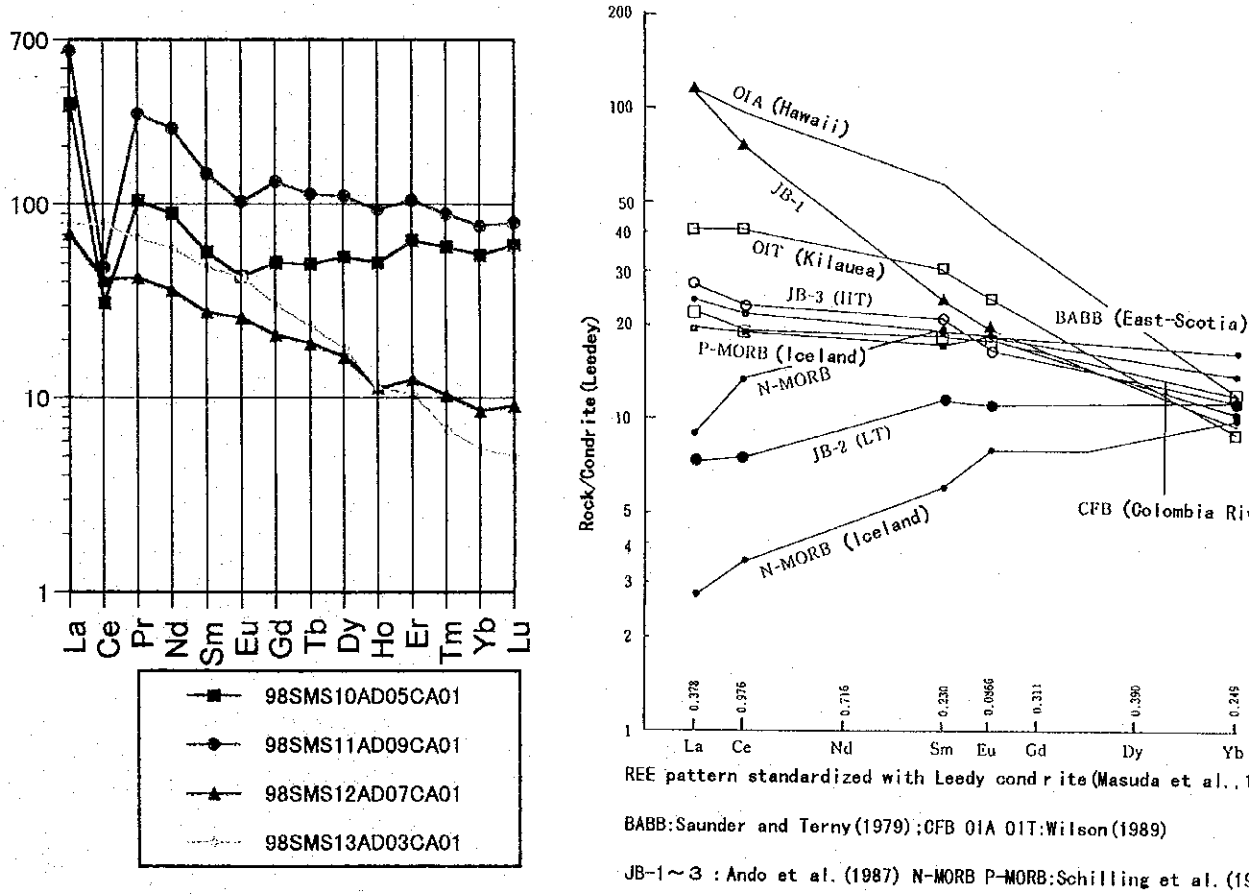

Fig. 4-4-4 Spidergram of REE elements

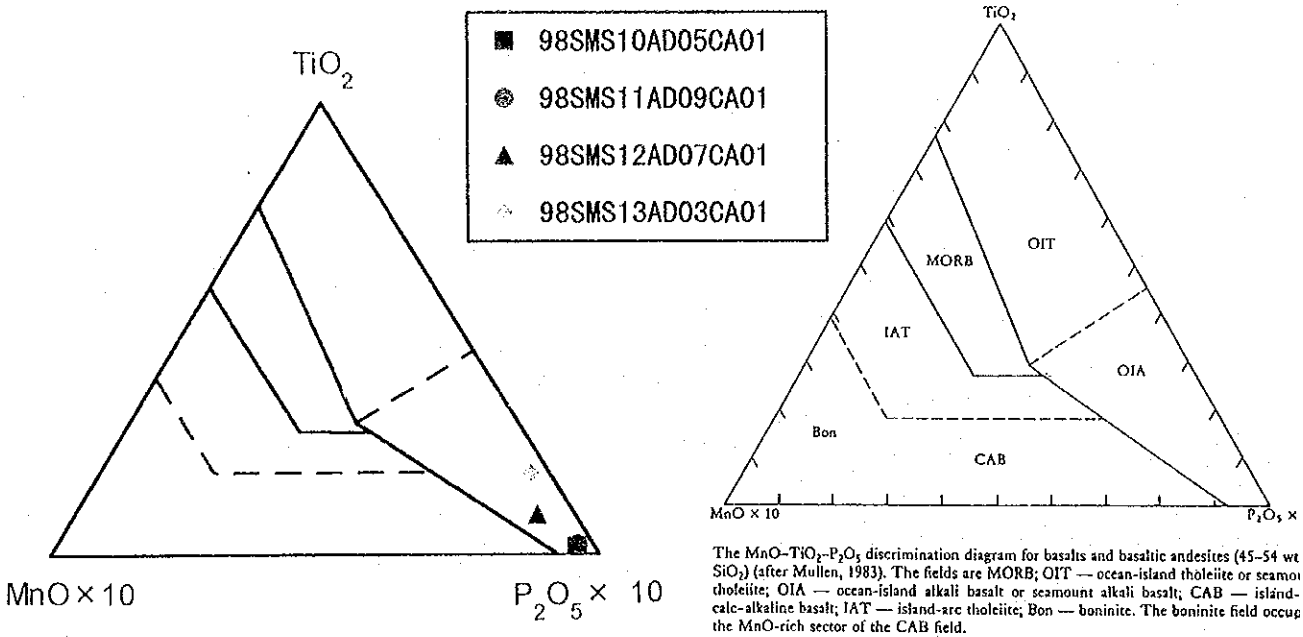

The MnO–TiO_2–P_2O_5 discrimination diagram for basalts and basaltic andesites (45–54 wt SiO_2) (after Mullen, 1983). The fields are MORB; OIT — ocean-island tholeiite or seamou tholeiite; OIA — ocean-island alkali basalt or seamount alkali basalt; CAB — island-calc-alkaline basalt; IAT — island-arc tholeiite; Bon — boninite. The boninite field occup the MnO-rich sector of the CAB field.

Fig. 4-4-5 TiO_2–MnO_2–P_2O_5 diagram

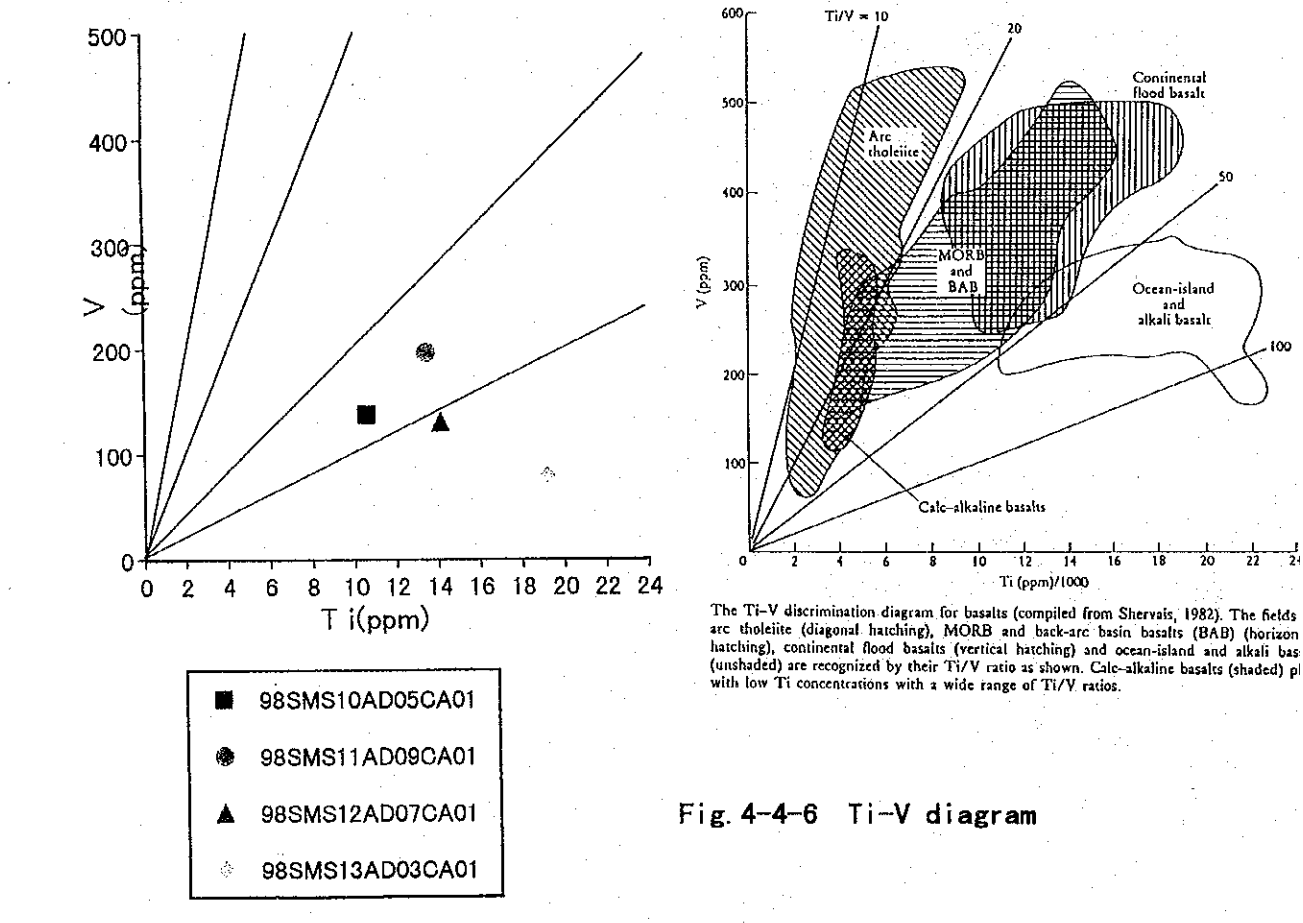

The Ti–V discrimination diagram for basalts (compiled from Shervais, 1982). The fields are tholeiite (diagonal hatching), MORB and back-arc basin basalts (BAB) (horizon hatching), continental flood basalts (vertical hatching) and ocean-island and alkali bas (unshaded) are recognized by their Ti/V ratio as shown. Calc-alkaline basalts (shaded) pl with low Ti concentrations with a wide range of Ti/V ratios.

Fig. 4-4-6 Ti–V diagram

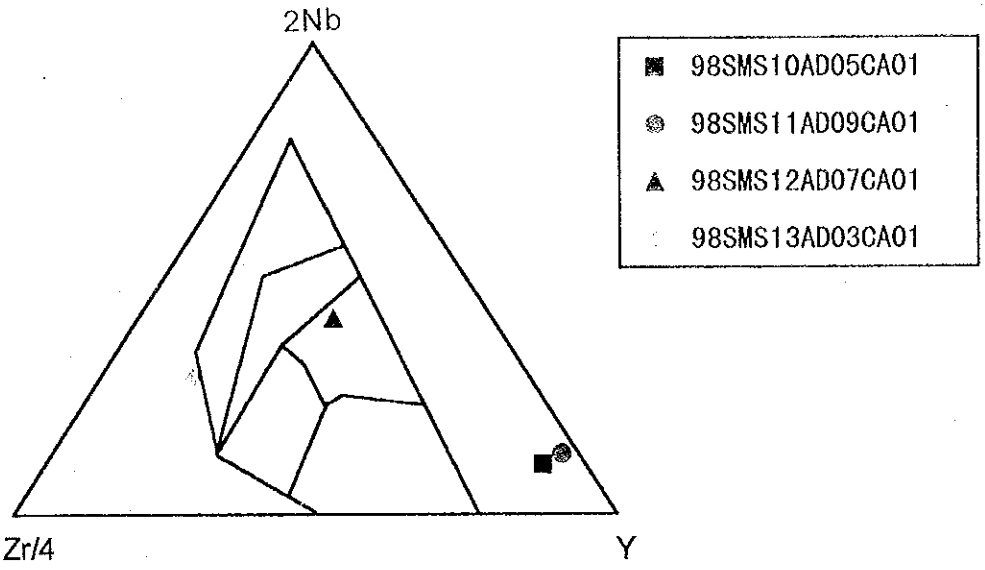

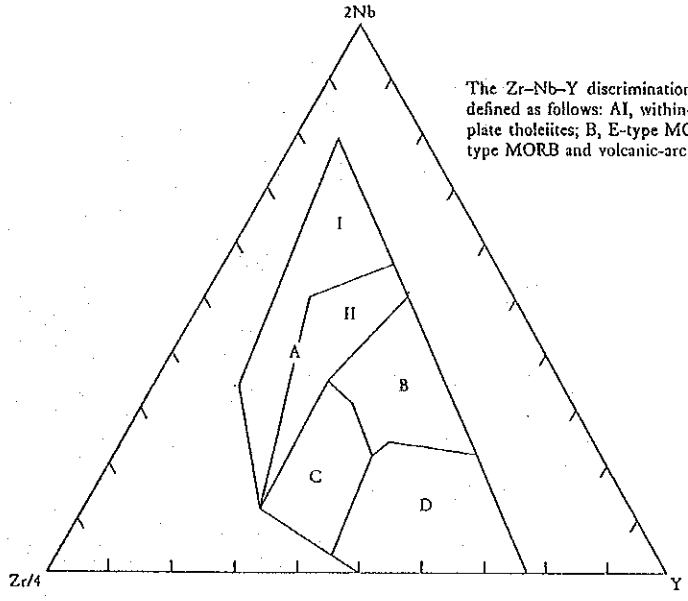

The Zr–Nb–Y discrimination diagram for basalts (after Meschede, 1986). The fields are defined as follows: AI, within-plate alkali basalts; AII, within-plate alkali basalts and within-plate tholeiites; B, E-type MORB; C, within-plate tholeiites and volcanic-arc basalts; D, N-type MORB and volcanic-arc basalts.

Fig. 4-4-7 Zn-Nb-Y diagram

Table 4-4-5 Classification of Basalt based on each diagram

area	Microscopic description	Normative composition diagram	AMF diagram	Spidergram of incompative elements	Spidergram of REE elements	TiO_2-Mn-P_2O_5 diagram	Ti-V diagram	Zn-Nb-Y diagram
MS10	Altered basalt	Olivine tholeiite	Tholeiite	OIA	OIA	OIA	out of domain	out of domain
MS11	Microphyric spherulitic olivine basalt	Tholeiite	Tholeiite	OIA	OIA	OIA	out of domain	out of domain
MS12	Basaltic pyroclastic rock	Tholeiite	Calc-alkali basalt	OIA	OIA	OIA	out of domain	E-MORB
MS13	Porous aphyric basalt	Tholeiite	Calc-alkali basalt	OIA	OIA	OIA	out of domain	out of domain

formed by hot spot volcanism and that the present arrangements of the islands and seamounts were completed by the movement of the Pacific Plate.

4 - 5 Identification of Fossils in Rocks and Bottom Sediments

Fossil identification was carried out for foraminifera, radiolaria, coral, and other biologic fragments in; six limestone and one tuff samples dredged, and one foraminiferal sand sample collected by LC sampling; a total of eight samples. The results of identification are shown in Table 4-5-1 and Table 4-5-2. The photographs of the typical foraminifera and radiolaria fossils are shown in Figure 4-5-1 and Figure 4-5-2 respectively. The microscopic photographs of fossils in thin sections are shown in Figure 4-5-3 . The samples used for this work were those recovered from areas MS10~12.

From MS13 area, foraminiferal calcareous conglomerate and tuff samples were collected, but those suitable for fossil identification were not obtained.

Table. 4-5-1 Results of fossil observation for rocks and seafloor sediments

Area	Sampling No.	Sample code	Sample No.	Sampling depth(m)	Sample classification	Foraminifera		Geological age	Radiolaria	Geological age	Coral	Geological age	others	Geological age
						Planktonic	Benthonic							
MS10	AD05	Fr02	A	1,506	Cray Filling volcanic pyroclastic rock									
	AD08	Fr01	E	1,325	Foraminifera calcareous	many		Middle Eocene						
	LC14	Fm04		1,468	Foraminifera sand	many		Late pliocene						
MS11	AD06	Fr02	I	2,284	Tuff	rare					unknown	unknown	Shell fragment	
	AD09	Fr01	B	2,425	Cray Filling volcanic pyroclastic rock	many		Middle Eocene					Shell fragment	
MS12	AD05	Fr01	A	1,629	Foraminifera calcareous	few	many	Middle Eocene			unknown	unknown	Sea-urchin	
	AD13	Fr01	A	1,626	Cray Filling volcanic pyroclastic rock	few					unknown	unknown		
		Fr02	A	1,626	Cray Filling volcanic pyroclastic rock	many		Middle Eocene						

The outline of the results are reported below.

From the seamounts of areas MS10~MS12, the materials filling the voids of foraminiferal limestone and reefal limestone contained middle Eocene planktonic foraminifera assemblage. Also micronodules were observed in these foraminiferal limestones. In the reefal limestone of MS12 seamount, neritic fossils such as; coral fragments, shell fragments, echinoidea thorns, and ostracoda were confirmed, but they were poorly preserved and the species and geological ages could not be determined. This reefal limestone, however, is contained in the foraminiferal

Table 4-5-2 Results of Fossil Identification in Rocks and Bottom Sediments

No.	Sampled locality	Sampling number	Sample number	Water depth (m)	Unaided eye observation	Identified fossils	Remarks
1	SMS10	AD05	Fr02	1506	Cray filling cruck of volcanic pyroclastic rock	not found	
2		AD08	Fr01	1325	Pelagic limestone, contain many angular fragments of Mn crust.	Contain many planktonic foraminifera, but no benthic forminifera. Major benthic foraminifera assemblage consists largely of genus *Truncorotaloides* with somewhat angular chamber and genus *Sulbotina* with rounded chamber while genus *Morozovella* with sha r p edges and lenticular from is not abundant. *Morozovella spinulosa, Truncorotaloides rohri, T.topilensis* are observed in thin sections. These 3 species appear at P11 and become extinct near the middle/late Eocene boundary (near the bottom of P15, 37.5～38.5 Ma)(Berggren et al., 1995).	The rocks dredged from the slope of this seamount (AD08, 1,325m) is located near the summit, but do not contain shallow sea fossils. This sample contains many manganese crust samples, and it is inferred that the bedrock of the seamount and the crusts on its surface and were mixed in the sample. Therefore, it is believed that the seamount was submerged quite deeply although above CCD in middle Eocene.
3		LC14	Fm04	1468	Small amount of black, opaque, irregularly formed minerals are included; probably Mn mineral or basalt fragments. Very small amount of colorless, transparent, polygonal, irregular minerals are contained, probably volcanic glass.	Planktonic foraminifera fossils assemblage in those sediments are; *Globigerinoides conglo batus, G.sacculifer, Gruber, Globigerinita glutinata, Globarotalia menardii, Neogloboquadrina dutertrei* (Table-3). This assemblage is considered to be of late Pliocene (1.77～2.0Ma) because it contains *Globerina nepenthes, Globerinoides obliquus extremus, Globerigerinoides fistulosus, and Globorotalia truncatulinoides.*	
4	SMS11	AD06	Fr02	2284	Contain fine-grained fragments of volcano-sedimentary corals and shells.	Fragments of corals and shells occur, but preservation is poor and identification of fossils difficult. But neritic fossils are definitely mixed. Planktonic foraminifera are observed filling the voids of coral fossils, but they are fragmentary and mere, impressions and the species cannot be determined.	The age of limestone dredged from the slope (AD09, 2,425m) of this seamount is also middle Eocene. AD06 (2,284m) does not contain fossils, and sediments derived from bedrock volcanic rocks are exposed. This indicates that this seamount walls also submerged to a depth of pelagic limestone formation during middle Eocene.
5		AD09	Fr01	2425	Pelagic limestone, contain many angular fragments of Mn crust.	Planktonic foraminifera fossils are rather poorly preserved, many genus *Truncoro taloides* and genus *Sulbotina* are observed, while genus *Morozovella* is not abundant. *Molozovella spinulosa* and *truncorotaloides topilensis* occur in this thin section, thus the age is believed to be mid-middle Eocene (P11～P15, 45.4～38.5Ma) and low latitude sedimentary environment.	
6	SMS12	AD05	Fr01	1629	Wackestone with matrix filled by foraminifera. Conglomerate consisting of subrounded～subangular several mm limestone pebbles.	Two types of pebbles; angular limestone pebbles containing shallow sea fossils such as shell fragments, echinoid thorns, ostracods, benthic foraminifers, and rounded black pelagic limestone pebbles containing planktonic foraminifera. These pebbles are stratified and occur concentrated in lamina. Matrix consists of calcareous sediments containing benthic or planktonic foraminifera sporadically. This is inferred to indicate the collapse and mixture of shallow sea limestone and pelagic limestone deposited around it. Mn crusts are formed on the surface of the pebbles and fossils, and thus it is inferred that there is a significant time interval between the formation of the pebbles and the mixing of the sediments. Regarding planktonic foraminifera, although in small number some fossils considered to be *Morozoella* and *Subbotina* are recognized. Thus the age is believed to be middle Eocene.	The rocks dredged from the slope of this seamount are divided into those containing fossil fragments of shallow sea (AD05, 1,629m) and those with volcanic pebbles (AD13, 1,626m). Those occur mixed in sediments containing middle Eocene fossils indicating the collapse and sliding down of parts of the seamount during this time. But the age of the volcanic rock forming the bedrock. It is thus clear that this seamount also submerged in Tertiary and was covered by middle Eocene pelagic calcareous ooze.
7		AD13	Fr01	1626	Cray filling cruck of volcanic pyroclastic rock	not found	
8			Fr02	1626	Pelagic limestone, containing angular 1cm volcanic pebbles.	Abundant planktonic foraminifera are contained in this sample, but benthic type are not observed. The major fossils assemblage is ; large amount of genus *Truncorotaloides* and *Marovella,* and small amount of genus *Subbotina* and *Acarinina*. Here, again, the occurrence of *Truncorotaloides rohri, T. topilensis*, and *M. spimulosa* indicate mid-middle Eocene (P11～P15, 45.5～38.5Ma) age and low latitude sedimentary environment.	

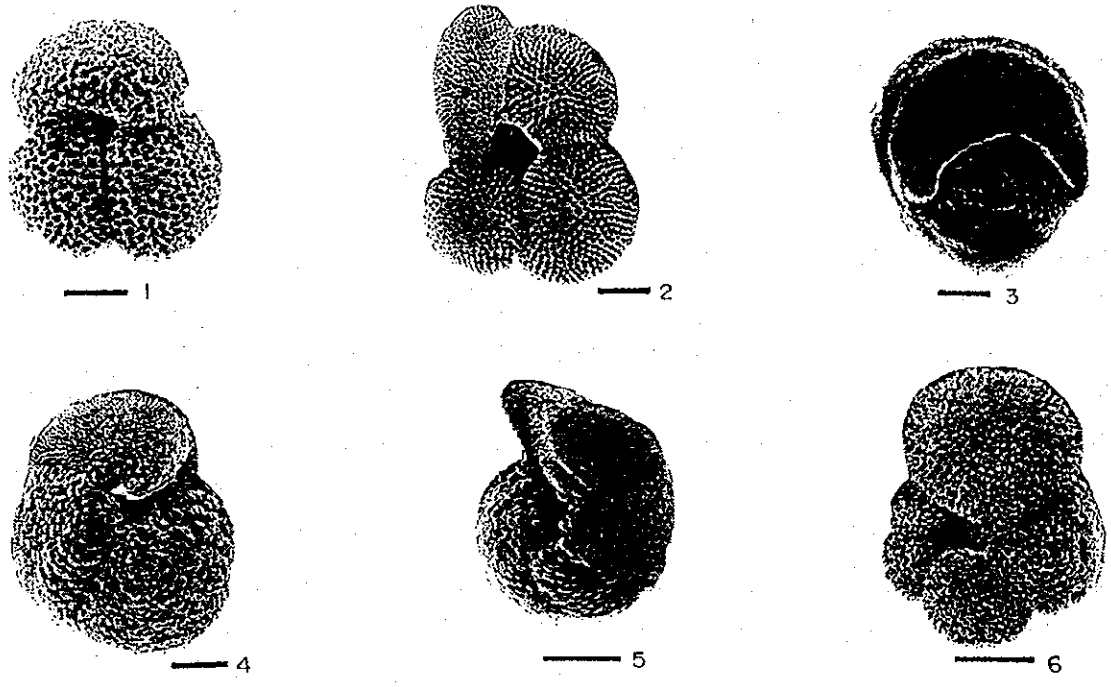

Scale bars: 100 μ m

1. Globigerinoides ruber (d'Orbigny). Umbilical view, Sample from 98SMS10LC14Fm04.
2. Globigerinoides sacculifer (Brady). Umbilical view, Sample from 98SMS10LC14Fm04.
3. Pulleniatina obliquiloculata (Parker and Jones). Umbilical view, Sample from 98SMS10LC14Fm04.
4. Globorotalia ronda Blow. Umbilical view, Sample from 98SMS10LC14Fm04.
5. Globorotalia truncatulinoides (d'Orbigny). Umbilical view, Sample from 98SMS10LC14Fm04.
6. Globigerinella aequilateralis (Brady). Apertural face, Sample from 98SMS10LC14Fm04.

Fig. 4-5-1 Species of the Typical Foraminifera Fossils

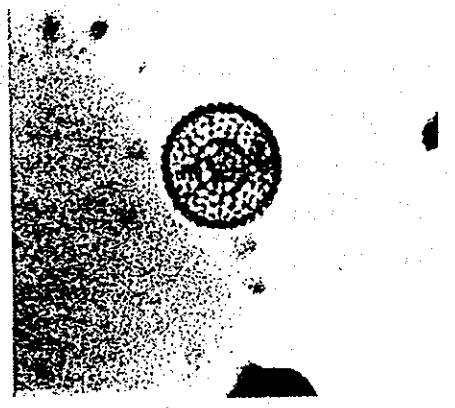

Thecosphaera sp.

98SMS10 LC14 Fm07

0.1 mm

Fig. 4-5-2 Species of the Typical Radiolarian Fossils

limestone as crust-coated pebbles and thus it was formed before Eocene. Tuff sample from upper slope of the MS11 seamount also contained coral and shell fragments, but they were fragmented, impressionized and species could not be determined. Fresh late Pliocene foraminifera fossils were confirmed in the foraminiferal sand recovered by LC sampling from immediately above the bedrock at the summit periphery of MS10 seamount.

The above results are interpreted as follows.

The seamounts of MS10~MS12 areas subsided during middle Eocene and their summits were at deep seafloor; there was a time lag sufficient for cobalt rich crust to grow to coating thickness between the completion of the above subsidence and the deposition of foraminifera which subsequently became foraminiferal limestone.

There is a possibility that coral reef was formed on the seamount of MS11, not only on MS12 seamount; the coral reef of MS12 was formed before middle Eocene; the MS10 seamount summit periphery was possibly exposed bedrock before late Pliocene.

From the above fossil identification results and age determination of rocks of the seamounts in the vicinity, the following history of the seamounts of the survey area is inferred.

The seamounts of the MS10~MS12 areas were formed during Late Cretaceous to early Paleogene as in the case of other seamounts in the vicinity. The summits of these seamounts were in shallow sea and flat summits were formed by wave erosion. Coral reefs were developed on the flat summits of MS11 and MS12 seamounts, but they gradually subsided and the summits were at deep seafloor by Eocene (37~58Ma). The seamount of the MS13 area is also considered to have undergone similar process of formation and subsidence from the rock samples and the crust thickness, but samples suitable for determining the age were not obtained during the present cruise.

The bottom sediment sample recovered from immediately above the bedrock 78cm below the depositional surface of the summit periphery of MS10 seamount contained late Pliocene (1.77~2.0Ma) foraminifera fossils. This fact indicates the existence of exposed bedrock before Pliocene. This does not necessarily indicate the existence of bedrock exposure from the completion of subsidence to Pliocene, but it does show that rocks were exposed for some length of time before Pliocene. This indicates the possibility of crust occurrence below the sediments. Also the sedimentation rate of unconsolidated sediments is low at 0.4mm per 1000 years, and the environment was favorable for crust growth.

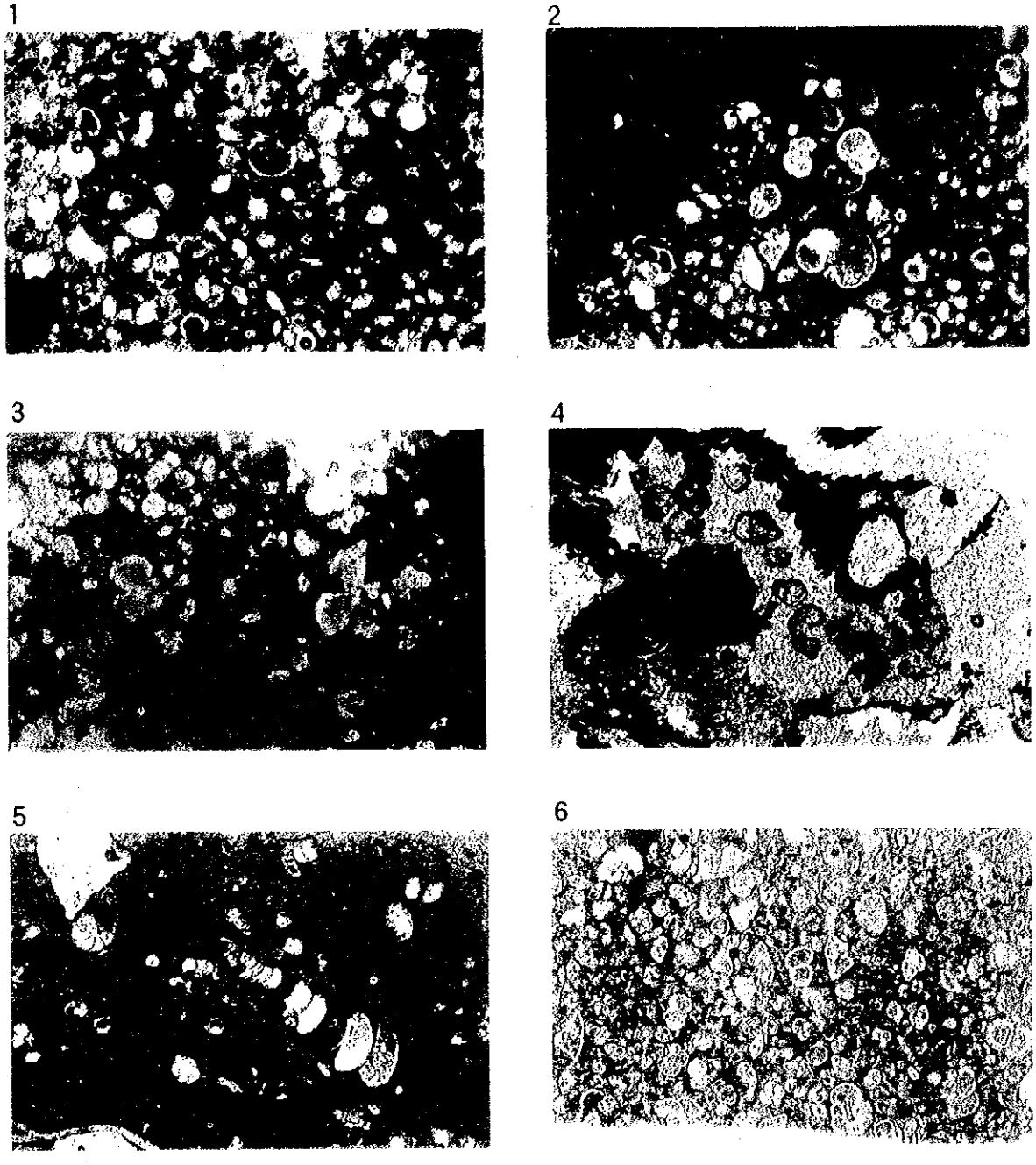

1. Planktonic foraminifera (Truncorotal oi des topilensis) Middle Eocene (98SMS10AD08)
2. Planktonic foraminifera (Subbotina Morozovella) Middle Eocene (98SMS10AD08)
3. Planktonic foraminifera (Truncorotal oi des topilensis, Subbotina Morozovella) Middle Eocene (98SMS11AD09)
4. Planktonic foraminifera (Subbotina Morozovella) Middle Eocene (98SMS11AD09)
5. Benthonic foraminifera (generic name unknown) (98SMS12AD09)
6. Planktonic foraminifera (Acarinina, Morozovella, Truncorotaloides, Subbotina) Middle Eocene (98SMS12AD13)

Fig.4-5-3 Photographs of microfossils in limestone and chart

4-6 Geological Summary of Each Area

1) MS10 area

The geology of this seamount consists of basalt and foraminiferal calcareous conglomerate on the summit and the slope. Tuff breccia is also distributed on the slope below 1,800m water depth. Basalt is vitreous and is classified as oceanic island alkali basalt. It is aphyric to microphyric with plagioclase, olivine, and augite phenocrysts. It is generally weathered strongly and clays fill the voids and cracks.

The foraminiferal calcareous conglomerate contains subangular to subrounded basalt pebbles, but those collected near the summit has almost all subrounded pebble. Microfossil identification confirmed planktonic foraminifera of near the boundary of middle Eocene to late Eocene (37.5~38.5Ma).

From the results of the present and past studies of the vicinity, it is concluded that the seamount of this area was formed by hot spot volcanism before middle Eocene (45.5~38.5Ma), and had subsided to the present water depth by late Eocene.

Regarding unconsolidated sediments, foraminiferal sand is distributed on the summit, and foraminiferal sand and calcareous clay are distributed below the lower slope. Rock exposures occur widely from the upper to middle slope. The sediments of the summit is thickest at the top of the dome attaining 50m, but they are several meters thick at the summit periphery. The Microsoft identification indicates the possibility that the peripheral parts were exposed before late Pliocene (2~1.77Ma).

2) MS11 area

The geology of this seamount consists generally of basalt. Also pelitic tuff is confirmed on the summit and foraminiferal limestone on the slope, but their distribution is limited.

Basalt is mostly olivine basalt and it is classified as oceanic island alkali basalt. It is aphyric to microphyric with plagioclase, olivine, and augite phenocrysts. It is generally strongly weathered and clays fill the cracks and voids.

In tuff, reefal coral fragments containing a large amount of calcareous clay were confirmed. This indicates that coral reef was formed on the summit , and that limestone probably occur below the sedimentary cover of the summit.

Middle Eocene (45.5~38.5Ma) foraminifera fossils were confirmed in foraminiferal limestone, and crusts are mixed and the subsidence of the seamount is believed to be before middle Eocene.

The seamount of this area is considered to have been formed by hot spot volcanism and was at a shallow depth suitable for reef formation. It subsequently subsided and reached the present water depth before middle Eocene (45.5~38.5Ma).

Unconsolidated sediments consisting of foraminiferal sand and calcareous clay are distributed throughout the seamount, but exposed rocks are observed near the summit pinnacles and parts of the upper slope.

3) MS12 area

Basalt and foraminiferal calcareous conglomerate generally occur on the seamount, and reefal limestone was confirmed on the summit. Also tuffaceous rocks were found to occur near the pinnacles on the summit and parts of the slope.

Basalt is mainly olivine basalt and is classified as oceanic island alkali basalt. It is generally aphyric, but samples with plagioclase, olivine, and augite phenocrysts were collected at the summit. It is generally strongly weathered and fresh samples were not recovered. Also basaltic hyaloclastite was observed, but its distribution is local.

Reefal limestone occurs widely on the summit in waters shallower than 1,600m. The age of the coral fossils is not clear, but it is inferred to have been formed before middle Eocene (45.5~38.5Ma). Middle Eocene foraminifera fossils have been confirmed from foraminiferal limestone.

The seamount in this area is considered to have been formed by hot spot volcanism, developed coral reef on the summit, and then subsided to the present water depth before middle Eocene (45.5~38.5Ma).

Unconsolidated sediments consisting of foraminiferal sand thickly covers the central part of the summit. Rocks are widely exposed from the summit periphery to the slope.

4) MS13 area

The major geologic units of the seamount of this area are basalt and foraminiferal calcareous conglomerate. Tuff breccia is also observed on the upper western slope.

Basal is mainly aphyric and is classified as oceanic island alkali basalt. Some minute phenocrysts of plagioclase, olivine, and augite are seen. It is generally strongly weathered and both the matrix and phenocrysts are argillized. Basaltic hyaloclastite occurs in the depressions between pinnacles.

Foraminiferal calcareous conglomerate contains large amount of angular basal pebbles, and the matrix is fragile merely cementing the pebbles.

The seamount of this area is considered to have been formed by hot spot volcanism and subsequently subsided to the present water depth. It was not possible to recover basalt samples sufficiently fresh for age determination, and limestone sufficiently fresh for fossil identification, and thus the age of these rocks are not known. But the REE pattern obtained by chemical analysis is similar to that of MS12 seamount, if the age of the two basalts is similar, the MS13 seamount was formed before early Paleogene.

Unconsolidated sediments consisting of calcareous clay containing foraminiferal sand cover most of the seamount, but exposed rocks are observed near the pinnacles which occur scattered on the summit.

Chapter 5 Cobalt-Rich Crusts

5 – 1 Classification and Layered Structure of Cobalt-Rich Crusts

(1) Classification of cobalt-rich crusts

The collected samples accompanied by cobalt-rich crusts are classified into the following three types; namely crust, cobble crust, and nodules. When the average thickness of the cobalt-rich crust is less than 1mm, they are classified as rock samples, and the term "coating" is used when the crust covers the whole sample and "stain" is used when the crust is merely attached locally. Also when the host rock is not confirmed, it is described as crust fragment.

Photographs of typical crusts are shown in Figure 5-1-1(1),(2).

① Crusts

Crusts are material whose upper surfaces and the sides are covered by cobalt-rich crusts and fresh substrates are exposed on the bottom surfaces. The substrates are mostly rocks, but in rare cases they are consolidated bottom sediments (clay).

The crusts are often separated from the substrates during sampling, and collected as crust fragments without substrates. These crusts are classified as "crusts" in calculating the amount of samples and other statistical purposes, but are separated from those with substrates as crust fragments" in description of each sample.

② Cobble crusts

Cobble crust is a cobble-shaped material, exceeding 8cm in long axis, and whose entire surface is covered by cobalt-rich crust. It has a nucleus consisting of rock and crust fragments, or other material. Those samples which can be shown to have clearly existed on the seafloor as cobbles from weathering and crust conditions are classified in this category regardless of exposed substrate on the bottom or sides.

Many nuclei are rocks, but some are crust fragments separated from the slopes and nodules. The crust is generally developed on the upper surface, and, as a rule, the surface with thick crust is defined as the upper surface in this survey.

③ Nodules

Nodules are material smaller than 8cm in diameter and are covered entirely by cobalt-rich crust. Nodules, similar to cobble crusts, have nuclei consisting of rock and crust fragments, some nodules do not have nucleus.

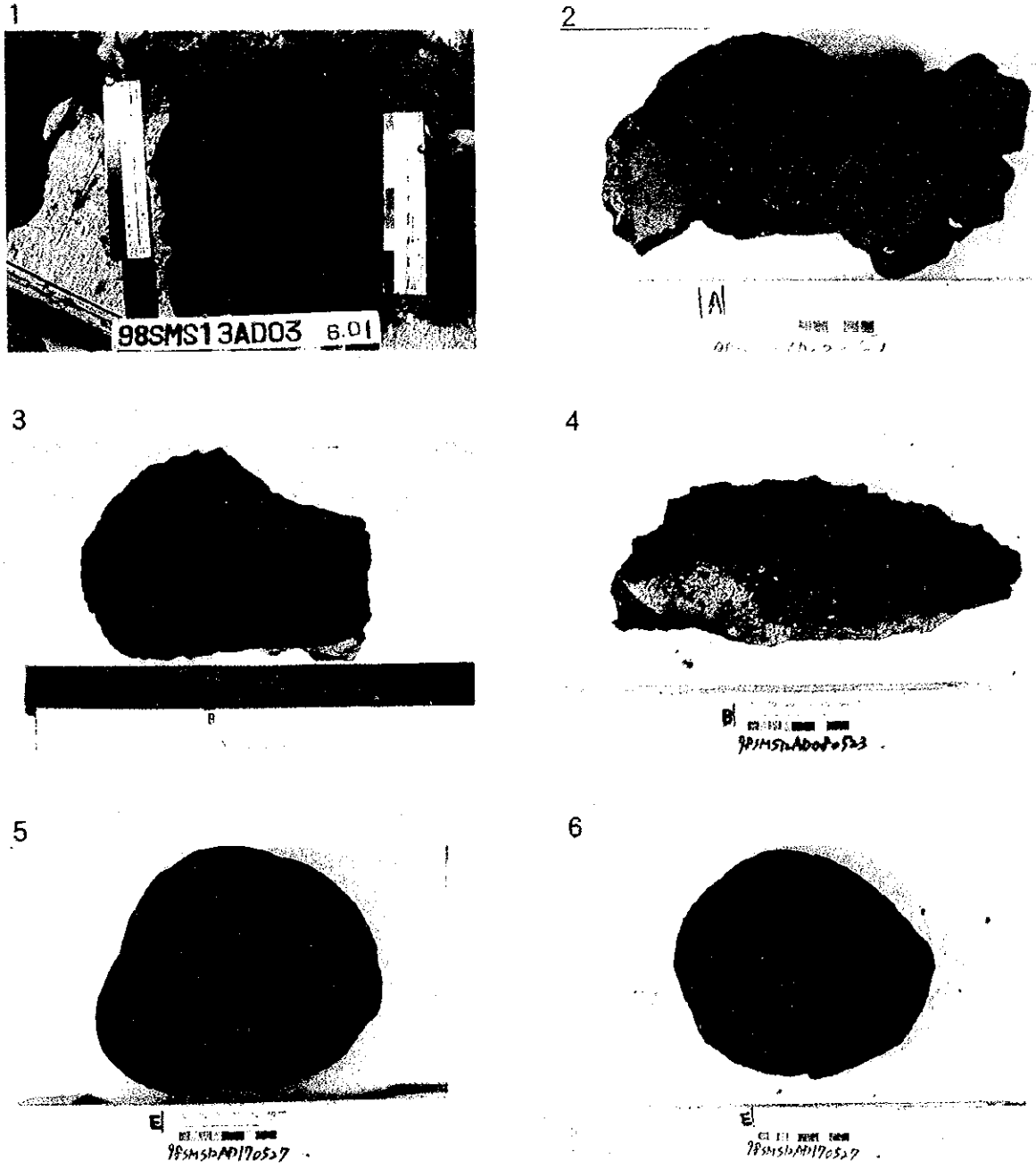

1. 98SMS13AD03-A Crust (upper) surface: botryoidal
2. 〃 Crust(Section) substrate:Basalt
3. 98SMS12AD08-B Crust (upper) surface: granullar
4. 〃 Crust(Section) substrate: Feraminifera limestone
5. 98SMC12AD17-F Cobble crust (upper) surface: botryoidal
6. 〃 Cobble crust(Section)substrate: Feraminifera calcareous conglomelate

Fig. 5-1-1(1) Photographs of cobalt-rich crust

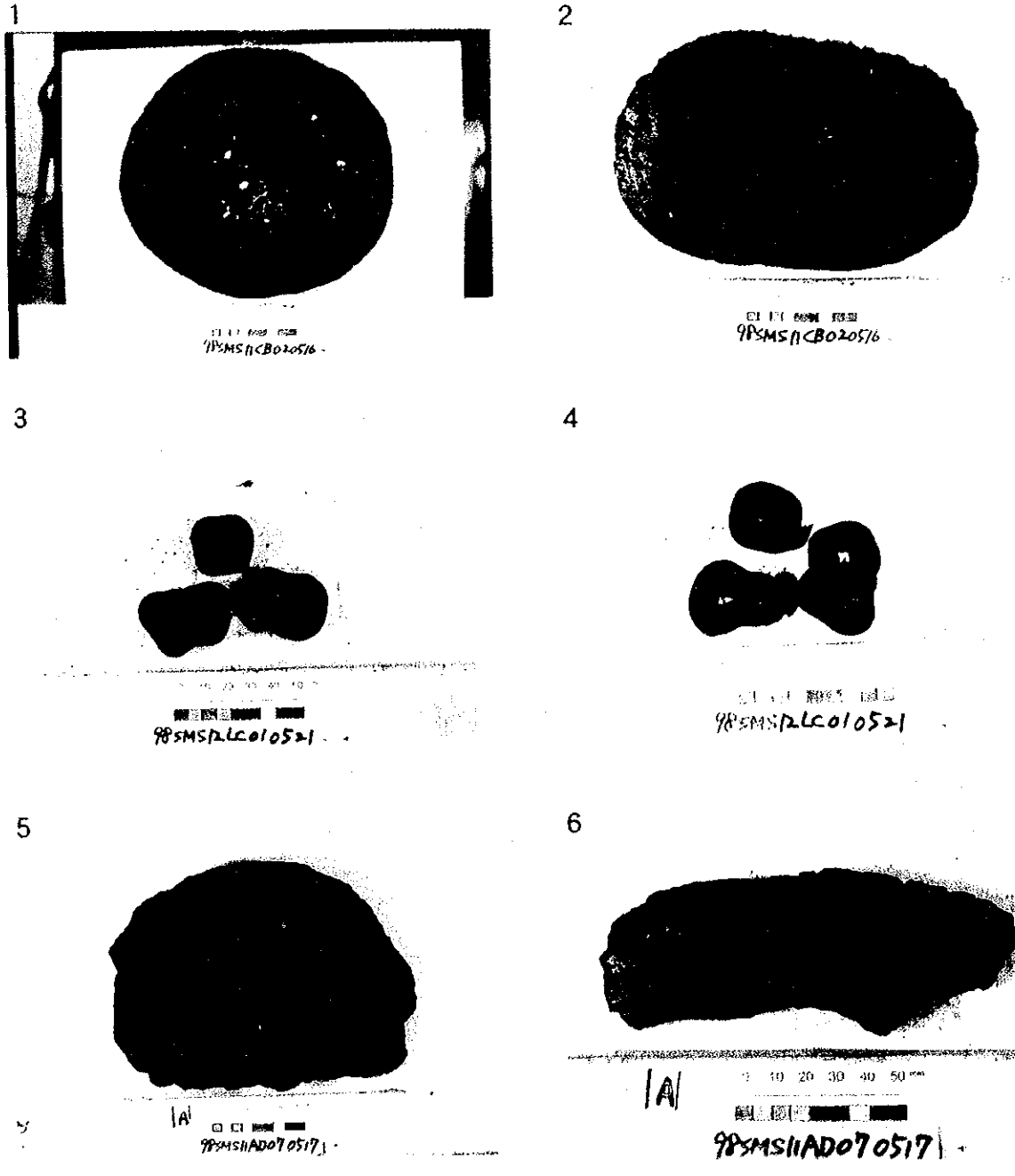

1. 98SMS11AD02-A Cobble Crust (upper) surface: botryoidal
2. 〃 Cobble Crust(Section) substrate: Fragment crust
3. 98SMS12LC01-F Nodule (upper) surface: smooth
4. 〃 Nodule (Section) substrate: limestone
5. 98SMS11AD07-A Fragment crust (upper) surface: botryoidal
6. 〃 Fragment crust(Section)

Fig. 5-1-1(2) Photographs of cobalt-rich crust

It is grouped into spherical, flat, platy, and irregular by shape.

(2) Thickness of crust

The thickness of the crusts is defined as; the thickness from the surface of the substrate to the crust surface in the direction of its growth of the crusts and cobble crusts. For crust fragments, the thickness is measured in the direction normal to the layered structure.

For those with substrates consistiing of crust fragments, the thickness includes that of the crust fragments. The thickness of the underside, however, is not included. The measurement is made in the growth direction of the cobalt-rich crust on the outer side or of the thicker part of the nuclei crust fragments.

Regarding the thickness of the nodules, nuclei to the surface is measured for those with nuclei, but short axis is used as thickness for the mono-layered nodules without nuclei.

The average thickness was determined as follows. The recovered material, after each sampling, was separated into crusts, cobble crusts, and nodules, and a sample considered to have average thickness within each group was selected and its value was used as the average of the group. The average thickness of the whole area was obtained by calculating the weighted average by multiplying the average thickness of each group by its surface area. In this report, the term "average thickness of the crusts" is used to denote the average of the combined thickness of both the crusts and cobble crusts.

(3) Division of the surface structure of the cobalt-rich crust

The surface structure of the cobalt-rich crusts is classified into three groups; namely botryoidal surface which is an aggregate of spherical to oval grains of several millimeters to 10mm in diameter, granular surface which is an aggregate of irregularly shaped minute grains, and smooth surface. Although it is difficult to determine whether the surface is granular or botryoidal in some samples, those with clearly shaped grains covering more than half of the surface is classified as botryoidal in the present survey.

Generally thick cobalt-rich crusts show botryoidal surface in many cases although those with granular and smooth surface is also observed.

(4) Layers of cobalt-rich crust

Many cobalt-rich crusts have two- to three-layered structure and some of those thicker than 50mm have more than four layers, and some with irregularly intercalated thin layers can be divided into seven to nine layers.

Structurally the crusts are divided as follows.

- Compact
  - Massive
  - Stratified
    - Non fissile
    - Fissile
- Porous
  - Scoriaceous
    - Prismatic voids developed
    - Spherical voids developed
  - Brick-like
    - Minute voids developed throughout the crusts
    - Minute voids distributed irregularly

Crusts are generally relatively hard, but some scoriaceous materials are soft and can be crushed by fingers. Also some have; intercalations of thin or thread-lace calcite, mixture of iron oxides, ooze and calcareous clay filling the voids, containing iron oxides. All the layers is believed to reflect; the age of cobalt-rich crust, genetic environment, difference of growth rate, and other relevant factors.

Generally with crusts and cobble crusts, thicker crusts tend to have larger number of layers, while nodules tend to be mono-layered. However, there are mono-layered crusts and nodules with several tens of millimeters and also thin crusts and nodules with several layers.

In the present study, most of the samples were analyzed in bulk, but also in a few cases they each layer was analyzed. The layers are numbered with the outermost layer as the first layer.

5-2 Results of Seafloor Observation

TV-mounted deep sea towing camera system (FDC) was used for clarifying the mode of occurrence of the cobalt-rich crusts of each area. The FDC track lines were designed after considering the results of; MBES acoustic pressure distribution maps, SSS survey results, and sampling by dredges. Clarification of; the mode of occurrence of the crusts, conditions of rock exposures and bottom sediments, and microtopography were the objective of this study.

Six track lines, one to two lines in each of the four areas, MS10~MS13, were surveyed.

Representative FDC seafloor photographs are shown in Figure 5-2-1(1),(2), FDC survey results in Appended Table 1, FDC route maps (plans and sections) and maps showing the crust exposure ratios are laid out in Appended Figure 5 (1)~(6).

The crust exposure ratio is the areal extent of the exposures of the cobalt-rich crusts, cobble crusts, and nodules on the seafloor without unconsolidated cover. It is expressed in percentage of the area surveyed, and it is shown in an average value during 30 second observation. The seafloor area observed by a single TV image is about 2m x 3m.

1) MS10 area

One FDC01 track line was surveyed in this area. This track line is located on the northwestern slope of the eastern part of the seamount, extending from the summit (1,400m water depth) to the middle slope (2,800m). The direction of the track line is northeast, and the total length of the observation is 2.5 miles. The results are shown in Table 5-2-1 (1).

Cobalt-rich crusts occur dominantly from the summit periphery to the upper slope (1,400~1670m). The exposure ratio is 80~90% and botryoidal crust surface is observed. AD05 sampling (1,445m) carried out across the FDC track line at the peripheral zone collected a crust sample with maximum thickness of 24mm and average 18mm.

The cobalt-rich crust exposure ratio is high at 80~90% on the upper slope with 1,670~2,000m water depth. Here, the crust surface is smooth to granular. Fissures and other surface features of the bedrock could be observed in some parts, and the crust could be thinner than at the periphery.

Talus deposits occur in the valleys below 2,600m water depth. Between 2,600m and 2,800m, cobble crusts with botryoidal surface occur mixed with the angular gravel of the talus.

2) MS11 area

One FDC01 track line was surveyed in this area. The track line is located on the eastern slope extending from the summit periphery (1,600m water depth)to the middle slope (2,900m). The direction of the line is northeast and the observed length is 3.2miles. The results of the observation is shown in Table 5-2-1 (2).

Table5-2-1(1) MS10FDC 01 Seafloor Observation Results

A water depth(m)	Topographic division	MBES acoustic pressure	Exposure ratio (%)	Geologic conditions	Crust conditions	Topography
1,350～1,400	Summit	Pale	0～30	Foraminiferal sand	Cobble crusts, nodules scattered in	
1,400～1,670	Summit periphery	Dark	70～90	Exposed crusts	Botryoidal surface, maximum thickness 24mm, average 18mm.	
1,670～2,000	Upper slope	Dark	80～100	Exposed crusts, parts believed to be bedrock.	Smooth～granular surface. Cracks in substrates observed in parts.	
2,000～2,200	Upper～middle	Dark	60～90	Angular fragments, cobble crusts.	Cobble crusts with granular surface observed.	Several-meters high cliffs continue.
2,200～2,500	Middle slope	Pale	0～20	Foraminiferal sand	Botryoidal crusts exposed in parts of 2,400～2,500m depth.	Ripple marks and trace fossils observed.
2,500～2,600	Middle slope	Pale	40～70	Deposits of angular fragment believed to be talus.	Angles of the cobble are clearly observed, possibly the crusts are mere coatings.	Steep cliff with several tens of meters relative height near 2,500m depth.
2,600～2,800	Middle slope	Pale	10～40	Mixture of angular rock fragments and cobble crust, covered by foraminiferal sand.	Cobble crusts with botryoidal surface.	
2,800～2,900	Middle slope	Pale	0～20	Foraminiferal sand	Angular fragments scattered. Crusts are believed to be mere coatings.	

Table5-2-1(2) MS11FDC 01 Seafloor Observation Results

A water depth(m)	Topographic division	MBES acoustic pressure	Exposure ratio (%)	Geologic conditions	Crust conditions	Topography
1,600～1,700	Summit	Pale	0	Foraminiferal sand		Scattered occurrence of sponges.
1,700～2,050	Summit	Dark	30～90	Foraminiferal sands cover crusts.	Crust surface botryoidal, cobble crusts scattered or foraminiferal sand.	Small cliffs continue near 2,000m depth.
2,050～2,440	Upper slope	Pale	0～30	Foraminiferal sand	Botryoidal cobble crust are scattered in some parts.	
2,440～2,700	Upper～middle slope	Intermediate	20～90	Foraminiferal sands thinly cover crusts and bedrock.	Although botryoidal crusts observed in some parts, outcrop surface is smooth and crusts, if any, are believed to be merely coatings.	Slope is relatively rugged.
2,700～2,900	Middle slope	Intermediate	0～40	Foraminiferal sands.	Although rock exposures and angular fragments are observed in some parts, surface is smooth and angles of rocks and cobbles are clear and crusts, if any, are believed to be mere coatings.	

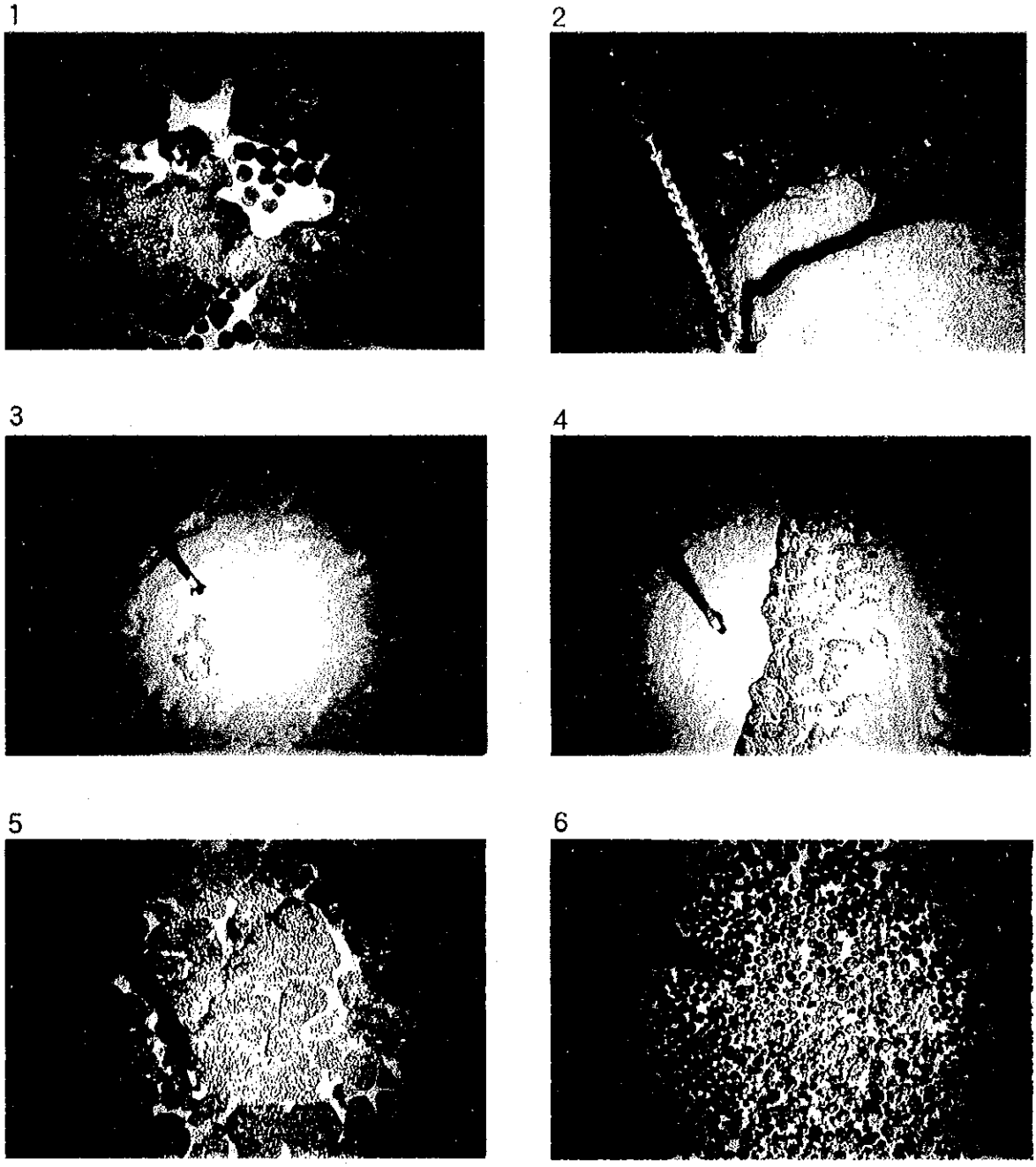

1. 98SMS10FDC01 Nodule and Cobble
   Summit Water depth 1,406m 12° 23.256'N 158° 39.626'E
2. 98SMS10FDC01 Steep-like outcrop of crust
   Upper slope Water depth 1,992m 12° 23.855'N 158° 40.516'E
3. 98SMS11FDC01 Foraminiferal sand with ripple mark
   Summit Water depth 1,633m 10° 57.318'N 161° 31.437'E
4. 98SMS11FDC01 Crusts covered by sand
   Middle slope Water depth 2,798m 10° 57.333'N 161° 33.792'E
5. 98SMS12FDC01 Crusts with pavement structure
   Summit Water depth 1,306m 08° 42.991'N 163° 10.364'E
6. 98SMS12FDC01 Nodules occupying 90% of the area
   Summit Water depth 1,328m 08° 42.962'N 163° 10.475'E

Fig. 5-2-1 (1) Photographs of FDC seafloor observation

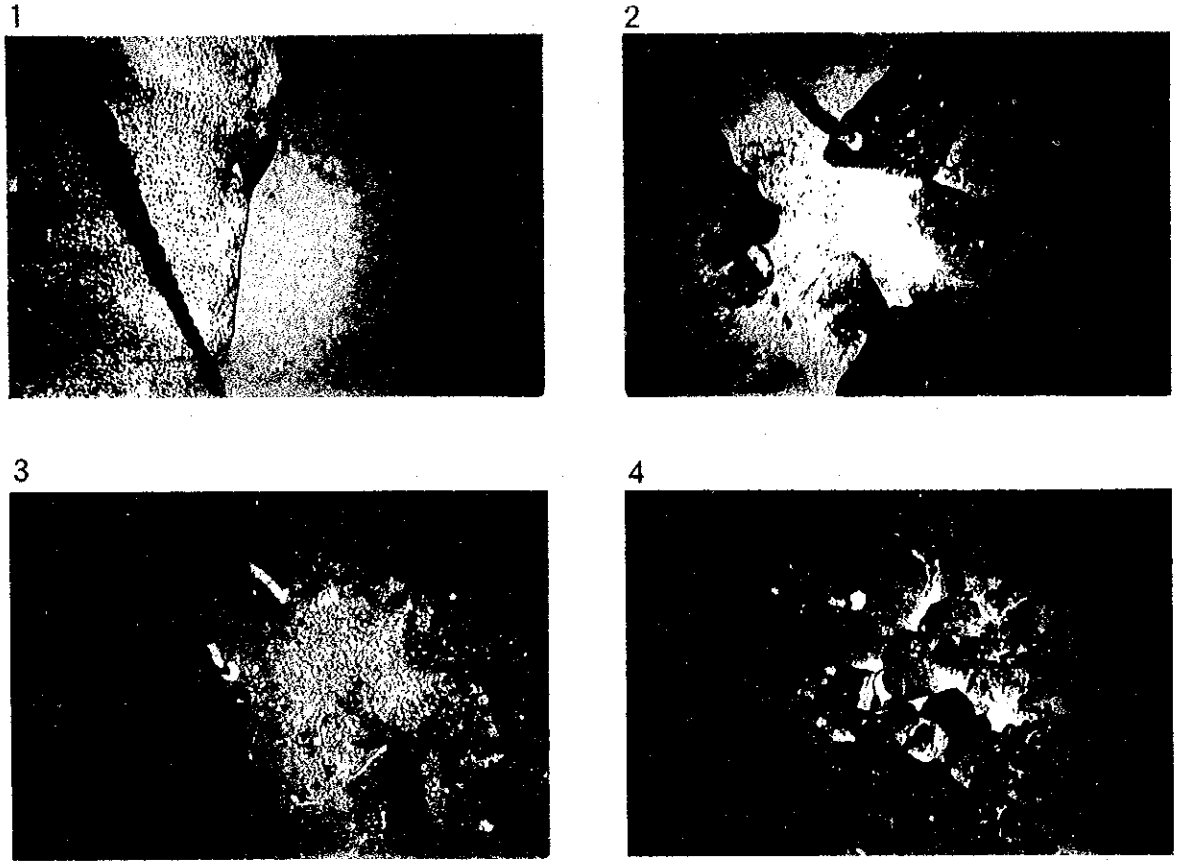

1. 98SMS12FDC02 Crust and Foraminiferal sand
   Summit Water depth 1,977m 08° 43.593'N 163° 16.941'E
2. 98SMS12FDC02 Cobble crust covered by sand
   Middle slope Water depth 2,436m 08° 43.547'N 163° 17.583'E
3. 98SMS13FDC01 Crust on slope
   Summit Water depth 1,554m 08° 10.186'N 160° 35.166'E
4. 98SMS13FDC01 Cobble crust and nodule
   Upper slope Water depth 2,962m 08° 28.150'N 160° 38.509'E

Fig. 5-2-1 (2) Photographs of FDC seafloor observation

Crusts with botryoidal surface are exposed at the summit periphery with 1,700~2,050m water depth. The exposure ratio is 30~90%. There are places where sediments are dominant and cobble crust with botryoidal surface occur sporadically in these localities.

The slope of this track line is gentle, and foraminiferal sand occurs dominantly. Botryoidal to smooth surface crusts are observed at protruded parts of the slope at 2,440~2,700m water depth corresponding to the upper to middle slope. This suggests the existence of crust under the foraminiferal sand.

3) MS12 area

Two track line were surveyed in this area. The track line FDC01 extends for 2.2 miles from the pinnacle slope (1,120m water depth) at the southern edge of the summit to the upper slope (1,420m). FDC02 extends for 2.4 miles from the summit (1,320m) of the eastern slope to the middle slope (2,560m). The results of observation are shown in Table 5-2-1 (3),(4).

Cobalt-rich crusts are observed on the pinnacle slopes and the peripheral parts of the summit.

Along FDC01, crusts with botryoidal surface are distributed continuously on the pinnacle slopes with exposure ratio of 60~95%. Crusts with botryoidal surface are distributed in the zone shallower than 1,370m of water depth, from the wide flat peripheral parts (1,300~1,330m deep) to the upper slope, but foraminiferal sand is dominant in some parts. Granular to bortyoidal cobble crusts and nodules occur sporadically on the foraminiferal sand in the peripheral parts. The zone below 1,370m becomes a steep cliff, and the cliff face is covered by smooth crusts.

Many cobble crusts were collected by dredging AD17 (1,273m water depth) carried out across FDC01. The maximum crust thickness is 95mm and average 32mm.

By FDC02, botryoidal crusts were confirmed at the summit periphery with water depth of 1,350~1550m. As in FDC01, parts of the crusts are covered by foraminiferal sand, and granular to botryoidal cobble crusts and nodules occur scattered over the sand.

Slope topography is an alternation of gentle slope and steep cliff. Angular gravel occur mixed with the foraminiferal sand on the gentle slopes and the occurrence of crust could not be confirmed. The steep cliffs also are often covered by angular gravel, but exposed parts are covered by smooth crusts. In some corners of the steep cliffs, botryoidal crusts are observed.

Table5-2-1(3) MS12FDC 01 Seafloor Observation Results

A water depth(m)	Topographic division	MBES acoustic pressure	Exposure ratio (%)	Geologic conditions	Crust conditions	Topography
1,120～1,300	Summit	Dark	60～95	Crusts are exposed, and partly covered by thin foraminiferal sands.	Crust have botryoidal surface.	
1,300～1,330	Summit periphery	Intermediate	35～90	Foraminiferal sand covers crusts, and cobble crusts, nodules occur on the sand.	Crusts and cobble crusts have botryoidal surface. Generally cobble crust exposures more pronounced than crusts. Many cobble crusts collected by sampling. Max 95mm. Ave 35mm.	Flat topography with slight depression.
1,330～1,370	Summit periphery～upper slope	Intermediate	0～50	Foraminiferal sand cover on crusts. Sand is generally thin with some thick parts.	Botryoidal crust surface.	
1,370～1,420	Summit	Dark	60～80	Exposed rocks.	Exposed surface is smooth and crusts, if any, are believed to be mere coatings.	Steep cliff over 50m in height.

Table5-2-1(4) MS12FDC 02 Seafloor Observation Results

A water depth(m)	Topographic division	MBES acoustic pressure	Exposure ratio (%)	Geologic conditions	Crust conditions	Topography
1,320～1,350	Summit	Pale	0～5	Foraminiferal sands.		
1,350～1,550	Summit periphery	Dark	40～80	Foraminiferal sands cover on crusts, Sand is generally thin with some thick parts.	Crust surface is botryoidal. Botryoidal or granular cobble crusts scattered on foraminiferal sand.	Small terraces continue on slope. Foraminiferal sand on terraces with 40～50%
1,550～2,450	Upper～middle slope		0～80	Angular fragments believed to be talus generally exist in the zone covered by foraminiferal sand.	Angles of the cobbles are clearly observed and crusts, if any, are believed to be mere coatings. Botryoidal crusts are partly observed on steep cliff, but the surface of the cliff is generally smooth and crusts are mere coatings, if any.	Terraced slope with alternating relatively flat and steep topography the steep cliffs are several tens to a hundred meters.
2,450～2,560		pale	0～10	Foraminiferal sands.	Several meters high cliffs with smooth exposures. Crusts are probably mere coatings.	Terraced slope with low steps and generally covered by foraminiferal sands.

4) MS13 area

Two track lines were surveyed. FDC01 extends for 2.2 miles from along the southern pinnacle slope on the summit (1,355~1,970m water depth), and FDC02 extends for 1.7 miles on the northern slope of the seamount. The results are laid out in Table 5-2-1 (5),(6).

The surface of the pinnacle slope in FDC01 is covered by crusts with granular to botryoidal surface. Botryoidal-surface and cobble crusts with maximum thickness of 60mm and average thickness exceeding 30mm were collected by dredging across the track line (AD09, 1,837m water depth).

Crusts and cobble crusts are confirmed at the summit periphery in FDC02 on the northern slope. The topography of the summit periphery consists of a series of stepwise terraces, and crusts with botryoidal surface are distributed on the slope, and cobble crusts occur sporadically on the foraminiferal sand deposited on the terraces.

The upper to middle slope is steep and crust is exposed over 80% of the area. Crusts with average thickness of 10mm were obtained from the western slope at the same water depth as FDC02.

5 - 3 Results of Sampling

Cobalt-rich crusts were sampled at MS10~MS13 areas by arm dredge (AD), chain bag dredge (CB) and large gravity corer (LC). Localities where the MBES images showed high acoustic pressure (high possibility of thin sediments and exposed cobalt-rich crusts on the seafloor) were targeted. The distribution of the sampling sites were designed to clarify the cobalt-rich crust occurrence of the entire seamounts by considering the results of the FDC observation, SBC, SSS, and sampling conditions. Sampling was carried out by the most effective method for each area by considering the characteristics of dredges and corer.

The total number of sampling sites was 61 in four areas; 49 dredge sites and 12 corer sites.

Thick crusts were recovered from all areas. Particularly in the three areas of MS10~12, thick crusts exceeding 20mm in average were collected from various localities from the summit periphery to the upper slope. From MS13 seamount in the southern part of the study area, many thick crusts exceeding several tens of millimeters to 100mm in thickness were collected. But the sites where thick crusts were recovered were limited.

Table5-2-1(5) MS13FDC 01 Seafloor Observation Results

A water depth(m)	Topographic division	MBES acoustic	Exposure ratio (%)	Geologic conditions	Crust conditions	Topography
1,430～1,355 ～1,520	Summit	Dark	20～100	Crusts exposed and covered by foraminiferal sands. Sand deposition is local.	Crust surface partly botryoidal, generally granular. Bedrock stratification observed and crust probably thin.	Pinnacle summits.
1,520～1,610	Summit	Dark	60～90	Crusts exposed, and covered by angular fragments and foraminiferal sands.	Crust surface granular. Angular fragments have clear angles and crusts, if any, are believed to be mere coatings.	Pinnacle slope.
1,610～1,670	Summit	Dark	30～100	Foraminiferal sands cover crusts.	Crusts with granular～botryoidal surface. Bedrock stratification and cracks observed and crusts believed to be thin.	Pinnacle slope.
1,670～1,970	Summit	Intermediate	0～60	Crusts observed in places, but foraminiferal sands cover the general zone and rock fragments and nodules occur sporadically on sand.	Crust surface granular.	Steep cliff over 50m in height.

Table5-2-1(6) MS13FDC 02 Seafloor Observation Results

A water depth(m)	Topographic division	MBES acoustic pressure	Exposure ratio (%)	Geologic conditions	Crust conditions	Topography
2,620～2,670	Summit	Pale	0	Ooze covering seafloor.		
2,670～2,740	Summit periphery	Intermediate	0～90	Ooze covering crust. Ooze generally thin with locally thick spot.	Crust surface botryoidal. Locally granular surface crust occur.	Steep cliff over 10m in height and.botryoidal surface crust one exist on it.
2,740～3,120	Upper slope	Dark	40～90	Generally crust exposing, locally some spot covered with sand. stebut locally. Steep criff which assumed landslide existing and large cobblescks are scattering.	Generally crust surface botryoidal and granular or smooth surface one exist on the criff. Large cobble are corted with crust.	Generally steep slope and cliff over 50m in height scattering.
3,120～3,200	Upper slope	Dark	0～40	Ooze covering crust.	Generally crust surface botryoida.	Some steep criff assumed landslide.
3,200～3,290	Upper slope	Intermediate	0～5	Ooze covering seafoor widely.	Locally, botryoidal surface crust exposing.	Steep cliff over 50m in height.

The following is a summary of the cobalt-rich crust samples of each area collected by dredges and corer. The sampling sites are shown in Figure 4-2-1(1)~(4). The results of sampling are shown in Appended Table 1 (1)~(4).

1) MS10 area

The average thickness of collected crusts and cobble crusts is 44.0mm (excluding nodules) with a maximum of 60mm for crusts and 115mm for cobble crusts.

Crusts and cobble crusts are distributed widely from the summit periphery to the slope of the seamount. The crust is thick from the summit periphery to the upper slope above 2,100m of water depth, the average thickness is over 60mm in the summit periphery and exceeds 24mm in the upper slope. Crusts exceeding 20mm in thickness were seen to occur continuously from the summit periphery to the upper slope in all directions, and over 50mm thick crusts were recovered from the summit periphery on the western side. Also the occurrence of crusts under foraminifera sand deposits was confirmed by LC at the eastern summit periphery where dredging was not carried out.

Thick cobble crusts mainly occur on the ridges of the southeastern edge of the summit, and many cobble crusts with thickness exceeding 50mm were recovered.

Most of the 20mm or thicker crusts have botryoidal surface, but some crusts thicker than 20mm with granular surface have also been collected from the upper slope. Although the number of sampling sites are not large on the northern slope, together with the results of FDC observation, it is believed that crusts thicker than 20mm occur on the upper northern slope where crusts with granular surface occur.

Many of the crusts have three to four layers. Those with compact first layer, porous second layer, and compact third layer are generally common throughout the seamount. The fourth layer is compact in some samples and porous in others. The cobble crusts generally have layered structure similar to that of the crusts, but some have compact second layer. The first layer is generally massive, but some cobble crusts from the upper southeastern slope have fissile layers.

2) MS11 area

The average thickness of the recovered crusts and cobble crusts is 38.6mm (excluding nodules) with a maximum of 140mm for crusts and 110mm for cobble crusts.

Crusts thicker than 20mm are distributed continuously from the eastern and western summit periphery to the middle slope. Particularly on the eastern slope; 140mm thick crusts were collected at the upper slope with 2,470~2500m water depth, and 90mm thick crust at the summit periphery with 1,760~1,950m water depth. FDC survey also confirmed the distribution of crusts with botryoidal surface from the summit periphery to the upper slope. Crust is also confirmed by large corer at the northeastern summit periphery where dredging was not carried out.

On the western slope, 20~35mm-thick crusts were mainly collected with a maximum of 50mm, but 110mm-thick cobble crusts were collected at the summit periphery.

It is a common feature of the crusts and cobble crusts that they have four to seven layers with compact and hard first layer, porous and fragile second layer. All layers from the third are compact and hard and some contain phosphates and/or concentrated iron oxides. Many of the crust fragments with thickness under 20mm are compact and hard corresponding to the first layer. Most of the samples collected on the southern and northern slope are compact and hard crust fragments similar to the above, however, the possibility of the occurrence of thick crusts in this zone is not small.

3) MS12 area

The average thickness of the recovered crusts and cobble crusts is 33.06mm (excluding nodules) with maximum of 96mm for crusts and 140mm for cobble crusts. In this seamount, crust thicker than 100mm were few, but those exceeding 50mm in thickness were collected from summit periphery to middle slope throughout the seamount with the exception of the eastern slope where sampling was not carried out. In other seamounts, crusts tended to be thicker on summit periphery than on the slopes, but here the difference in thickness was not observed between the above two topographic locations. FDC observation was carried out for the eastern slope where dredging was not done, and the continued occurrence of crusts with botryoidal surface was confirmed from the summit periphery to the upper slope above 1,550m water depth. Crusts with botryoidal surface was also observed in zones deeper than 1,550m, but the slope is covered by colluvium and the continuity of the crust could not be confirmed. LC sampling was attempted at the

summit periphery the occurrence of crust was confirmed, but detailed nature could not be clarified.

Crusts thicker than 20mm were collected also on pinnacle slopes on this seamount. FDC observation also confirmed that other pinnacles slopes on this summit are covered by crusts with botryoidal surface.

The crusts and cobble crusts have three to four layered structure. All layers of those collected from the southern slope and southern part of the western slope are compact while those from the northern part of the western slope and northern slope are porous.

4) MS13 area

The average thickness of collected crusts and cobble crusts is 46.4mm (excluding nodules) with a maximum of 140mm for crusts and 160mm for cobble crusts.

This is a rugged seamount topped by pinnacles, and MBES acoustic pressure images show that, with the exception of near the pinnacles, the summit and the eastern and southern slopes are covered by thick sediments. Sampling was carried out near the pinnacles and the slope on the western and northern side.

Dredging was done at four sites on the slope, only crustal coating was collected at three sites, but FDC seafloor observation confirmed the distribution of crusts with botryoidal surface from the summit periphery to the upper slope. Also 35mm-thick crust and 40mm-thick cobble crust was collected by AD03 on the northwestern side.

Near the pinnacles at the summit, crusts and cobble crusts thicker than 20mm were collected at all sites near the pinnacles. Many samples exceeding 100mm in thickness were collected near the pinnacles on the southwestern part of the summit and the average thickness is over 60mm. Occurrence of crusts was confirmed by FDC even in the vicinity of the pinnacles where dredging could not be carried out. Also it is inferred from the results of the SBP and SSS surveys that the sediments between the pinnacles are thin, and the existence of consolidated material under the thin calcareous clay was confirmed by large corer sampling. Thus the possibility of the occurrence of crusts in this zone is high.

Most crusts and cobble crusts have four-layered structure, and they are; compact first layer, porous second layer, compact third layer, and the fourth layer is very compact with vitreous luster.

5 - 4 Chemical Composition of Ores

Forty-eight cobalt-rich crust samples were selected from those collected at 43 sites in four areas of MS10~13. They were chemically analyzed. Crusts of 14 of these samples were separated into layers and each layer was analyzed, and the relation of the layered crust structure and chemical composition was studied. Total number of analysis was 106 samples.

Samples with thick cobalt-rich crusts were selected for bulk analysis from the crusts and cobble crusts with typical layered structure. As a rule, samples with substrates attached were used, but when crusts and cobble crusts were not available crust fragments and nodules were analyzed. The results of chemical analysis are laid out in Appendix Table 4 (1)~(3).

(1) Analyzed elements and analytical methods

The analyzed elements and analytical methods are shown in Table 5-4-1, and the analyzed elements and the limits of detection in Table 5-4-2. The samples were dried to constant weight before analysis and then the samples were prepared.

Table 5-4-1 Elements and Methods of analysis

Elements	Methods
Mn, Fe, Ti, Si, Al, Ca, P, Co, Ni, Cu, Pt	ICP emission spectrometry
Pb, Zn, V, La, Ce, Pr, Nb, Sm, Eu, Gd, Tb, Dy, Ho, Er, Tm, Yb, Lu	ICP mass spectrometry

Table 5-4-2 analyzed elements and the limits of detection

Elements	Limits of detection
Co, Ni, Cu, Mn, Fe, Pb, Zn, Ti, Mo, V, Si, Al, Ca, P	0.01%
Pt, Pd, La, Ce, Pr, Nb, Sm, Eu, Gd, Tb, Dy, Ho, Er, Tm, Yb, Lu	0.1ppm

(2) Chemical composition

The results of analysis of five major elements and platinum, and rare earth elements of the samples from various areas are laid out in Table 5-4-3. A radar chart of the five major components of the cobalt-rich crusts are shown in Figure 5-4-1. The relation between the water depth of the sampling sites and the grade is shown in Figure 5-4-2 .

Table 5-4-3 Results of Crust analysis

Area	Co %	Ni %	Cu %	Mn %	Fe %	Pt ppm	total REE ppm	Mn/Fe
MS10 area ave.	0.686	0.474	0.048	21.080	14.419	0.667	1453	1.48
MS11 area ave.	0.693	0.480	0.051	21.725	14.905	0.610	1700	1.47
MS12 area ave.	0.674	0.556	0.045	23.879	14.396	0.466	1762	1.70
MS13 area ave.	0.502	0.387	0.039	20.751	16.872	0.365	1650	1.24
MS area ave.	0.642	0.481	0.046	21.987	15.055	0.525	1636	1.49

The average grade of the five major elements of the cobalt-rich crusts from areas MS10 and MS11 is very close. The grade of the crusts from MS12 area is similar to these two areas, except Ni, Mn values are slightly higher. The grade of the samples from MS13 area is lower in Ni, Cu and higher in Fe. The chemical characteristics of the samples recovered this year are summarized as follows.

- Co grade varies considerably by the sampling site in all seamounts. Relation of the cobalt grade with the water depth is not clearly noted, but a very low grade samples were collected from the lower part to the foot of the slope.
- Ni grade variation is small with the exception of MS12 area. Samples with Ni grade higher by 1.5~2 times the average was collected at the northern periphery and near the pinnacles in the southern part of the summit. The grade tends to decrease with water depth.
- Cu grade varies considerably by the sampling sites in all seamounts. Content of some samples was below the limit of detection. Correlation between the water depth and grade is not observed. Samples containing three to four times the average Cu grade were obtained from MS10 and MS12 areas, the analyzed samples are nodules from the foot of the slopes deeper than 4,500m.
- Mn grade varies considerably by the sampling sites in all areas. The grade tends to decrease with water depth.
- Fe grade variation by sampling sites is somewhat smaller in MS11 and MS13 areas whereas it is large in

MS10 and MS12 areas. Generally the average grade tends to increase with water depth.

- Zn grade tends to decrease with water depth, while that of Ti tend to increase with depth. The Pb, Zn, Mo grades of samples from lower slope and the foot of seamounts are very low.
- Pt grade varies considerably by sampling sites. Correlation between the water depth and grade is not observed.
- Grades of total REE varies widely by the sampling sites. With the exception of two samples from 4,500m depth, the grade tends to increase with water depth.

(3) Local characteristics

Chemical characteristics of cobalt-rich crusts by areas are summarized below.

- MS10 area has the highest Pt content and Co, Cu grades are also high among the four areas. High Ni samples were also collected. Fe and total REE contents are the lowest in the four seamounts.
- MS11 area has the highest Co, Cu grades among the four areas. Ni, Mn, Pt, total REE grades are also high.
- MS12 area has the highest Ni, Mn, Pb, Zn, Ti, Mo, V, and total REE grades among the four areas.
- MS13 area has the highest Fe grade among the four areas. Co, Ni, Cu, Mn, and Pt grades are the lowest in the four seamounts.

(4) Results of layer analysis

Of the samples analyzed chemically, each layer of 14 samples was analyzed separately. Samples with three to seven layers were used. The average grades of the layers are laid out in Table 5-4-4. Co, Ni, Mn grades of these samples tend to increase outward from the inner layer and Cu and total REE contents tend to decrease outward. Similar trend is observed in the compact and porous layers, and Pt grade of porous layers tend to be higher.

Table 5-4-4 Results of layer analysis

Layer	Co %	Ni %	Cu %	Mn %	Fe %	Pb %	Zn %	Ti %	Mo %	V %	Si %	Al %	Ca %	P %	Pt ppm	total REE ppm
First layer	0.986	0.546	0.019	26.06	14.08	0.15	0.07	0.86	0.064	0.058	2.44	0.52	3.06	0.55	0.26	400
close	1.002	0.554	0.012	26.60	14.13	0.16	0.07	0.84	0.066	0.060	2.26	0.46	3.23	0.61	0.25	406
porous	0.918	0.512	0.069	23.71	13.85	0.13	0.06	0.94	0.052	0.050	3.25	0.76	2.34	0.29	0.29	372
Second layer	0.623	0.500	0.030	23.80	16.04	0.14	0.08	1.09	0.049	0.058	2.68	0.70	4.37	1.06	0.49	403
close	0.700	0.555	0.038	25.44	15.33	0.15	0.08	1.03	0.061	0.061	2.15	0.50	4.07	0.91	0.44	424
porous	0.564	0.458	0.024	22.56	16.57	0.14	0.07	1.13	0.041	0.056	3.08	0.85	4.58	1.18	0.52	387
Third layer	0.599	0.580	0.051	24.54	13.65	0.12	0.08	0.91	0.061	0.058	1.90	0.53	4.89	1.12	0.42	432
close	0.599	0.600	0.047	25.23	13.45	0.12	0.08	0.85	0.066	0.060	1.42	0.36	5.27	1.26	0.37	448
porous	0.600	0.518	0.062	22.47	14.25	0.10	0.08	1.11	0.045	0.052	3.32	1.04	3.76	0.70	0.58	386
Fourth layer	0.352	0.454	0.069	19.94	12.45	0.10	0.07	0.63	0.056	0.056	1.47	0.43	10.24	2.82	0.52	423
close	0.359	0.489	0.063	20.57	11.94	0.10	0.07	0.61	0.059	0.056	1.30	0.38	10.40	2.78	0.46	416
porous	0.332	0.348	0.086	18.03	13.96	0.09	0.07	0.70	0.046	0.055	2.00	0.59	9.74	2.96	0.69	443
Fifth layer	0.329	0.427	0.060	21.08	12.28	0.12	0.07	0.77	0.051	0.057	1.78	0.49	10.22	2.98	0.39	413
Sixth layer	0.212	0.259	0.050	15.35	12.72	0.13	0.06	0.67	0.040	0.056	1.58	0.41	13.70	4.42	0.35	428
Seventh layer	0.370	0.437	0.062	20.86	10.29	0.12	0.08	0.66	0.048	0.053	1.32	0.41	12.99	3.20	0.51	487

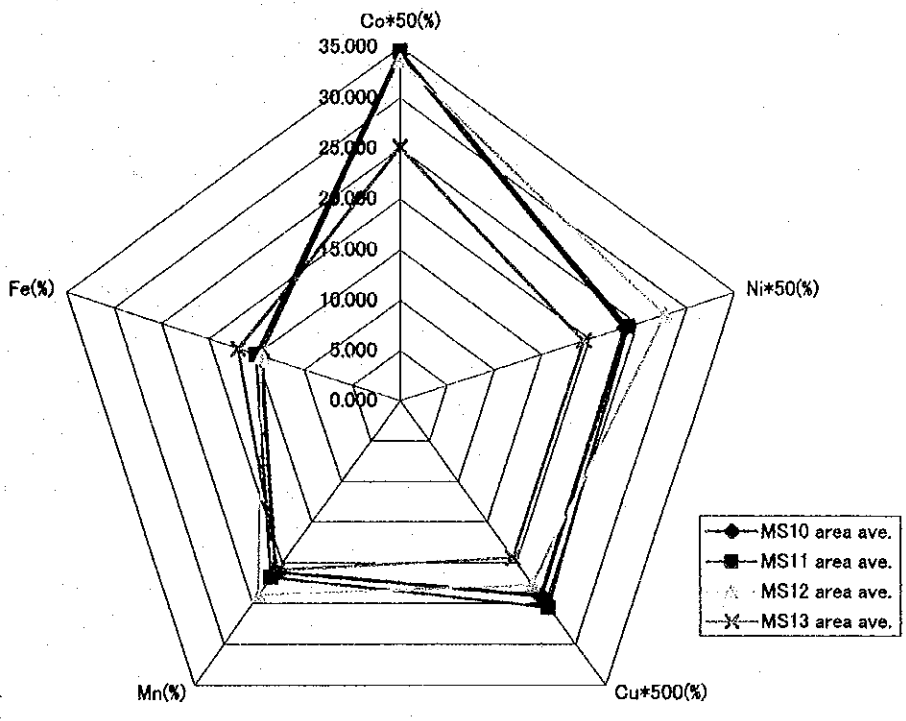

Fig.5-4-1 Comparison of five principal components

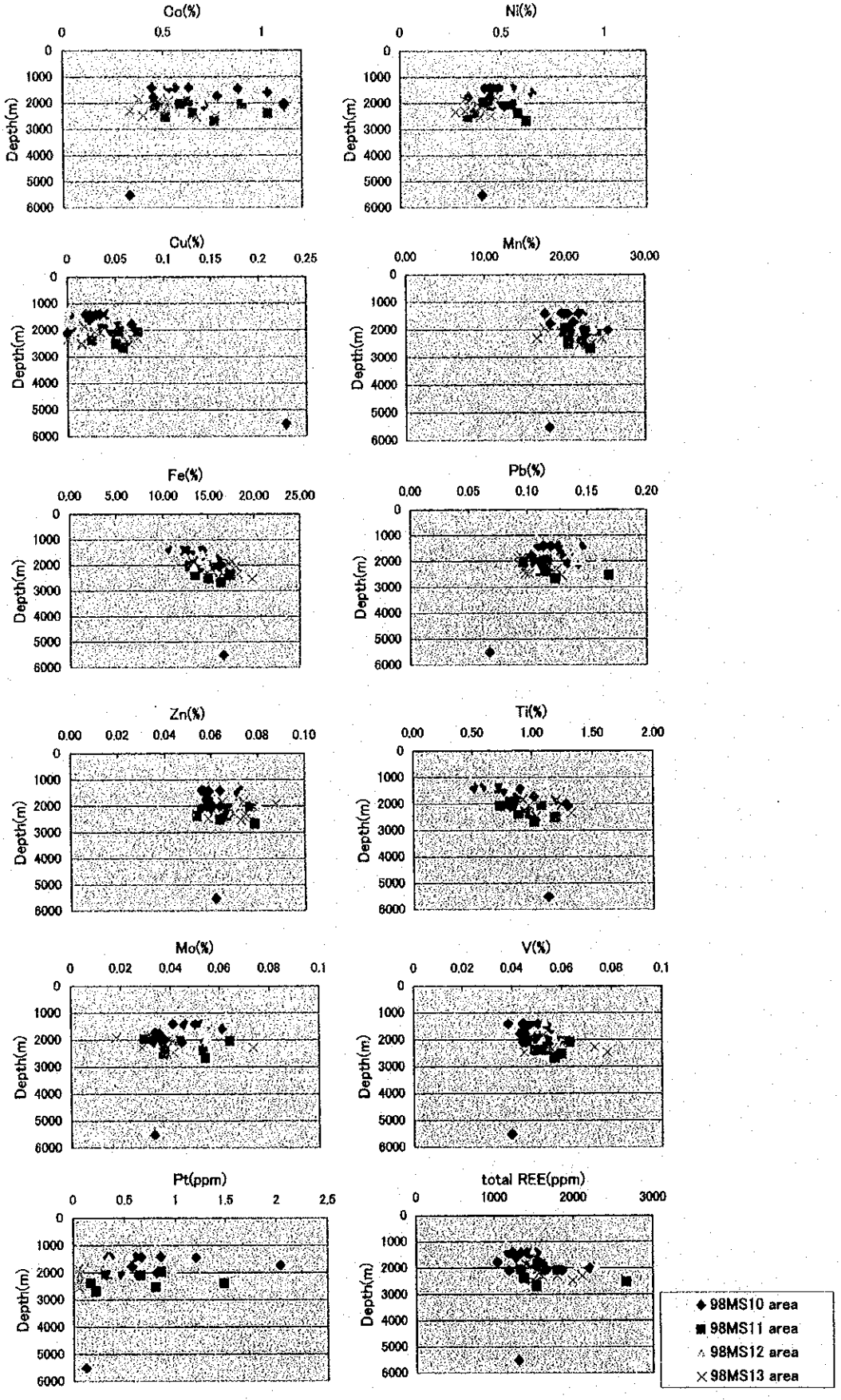

Fig.5-4-2 Sampling depth and concentration of each element

5 - 5 Mineral Composition

One of the sections of sample CB02 (southwestern periphery of summit, 2,019~1,902m water depth) from MS11 area contained 1~2mm thick blackish gray layer with metallic luster. Such layers do not occur commonly in cobalt-rich crusts, and this is the only sample in the present survey. Polished sections of this sample were prepared and microscopic observation and EPMA analysis was attempted. Line analysis was carried out simultaneously and examined the chemical variation.

(1) Analyzed sample

The sample has basalt nucleus which is covered by black manganese mineral. The cobalt-rich crusts has a three-layered structure with; compact and hard inner layer, compact and hard and iron oxide-bearing middle layer, and outer layer which is hard without impurities. And the middle layer ca be further divided into four sublayers and the outer layer into two. The thickness and description of the layers are laid out in Table 5-5-1.

The number of analysis is; ① point quantitative analysis at five points, ② qualitative line analysis for a length of 40mm. The analyzed points are shown in Figure 5-5-1.

The ore was cut by diamond cutter, thin section prepared, carbon was vapor deposited on the surface. The description of the thin sections is in Table 5-5-2.

(2) Results of chemical analysis

Analytical results are listed in Appendix Table.

Point qantitative analysis was carried out at a total of five points; namely three points in thin section 1, one point each in sections 2 and 3. The results of analysis are in Table 5-5-3. Triangular diagram with components of; Mn, Fe, and (Cu+Ni+Co) *10 is shown in Figure 5-5-2.

The line analysis for thin section 1 was carried out by beam diameter of 8000MS, and 396 point measurements were carried out with 100.15 μ m intervals. The analytical results are shown in Table 5-5-4, and the composition variation over the line analysis in Figure 5-5-3. It should be noted that the variation of grade is inferred from the quantitative point analysis and the accuracy is not as high as the point analysis.

Table 5-5-1 Description of sample

No.	Part		Thickness(mm)			Description
			Max.	Min.	Ave.	
1	Subtract		80	30	50	Microphyric basalt.Pyroxene fine phenocript scattering, but many of then altered to clay mineral.
2	Innermost		27	10	18	Composed with blackish and hard manganese mineral. Matrix texture is very close. Some blackishi-gray layer which thickness is 1-2mm Exist.
3	Inner	In4	5	3	4	Blackish and hard manganese mineral layer. orthophosphoric minerals scatterig.
4		In 3	11	5	7	Blackish and hard manganese mineral layer. Including iron oxide.
5		In 2	8	0	4	Blackish and hard manganese mineral layer. Discontinuity layer.
6		In1	9	3	5	Blackish and hard manganese mineral layer. orthophosphoric minerals scatterig.
7	Outer	Out 2	13	0	3	Blackish~brownish and porous texture. Calcareous cray filling pore-space.
8		out1	15	3	10	Very hard manganese crust layer, and show creavage texture.

Table 5-5-2 Description of thin section

sample	Description
1	Colloform texture of manganese mineral composing stratification structure. Partially, some course-grained minera found.
2	Colloform texture of manganese mineral composing stratification structure and show striped pattern.
3	Colloform texture of manganese mineral composing stratification structure. But structure is not clear comparing other samples.

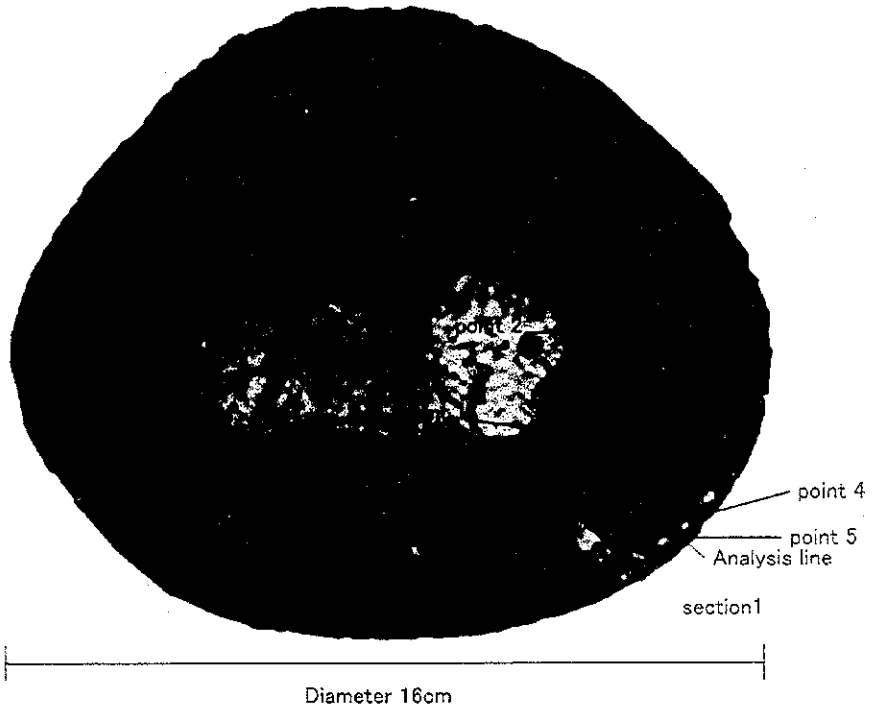

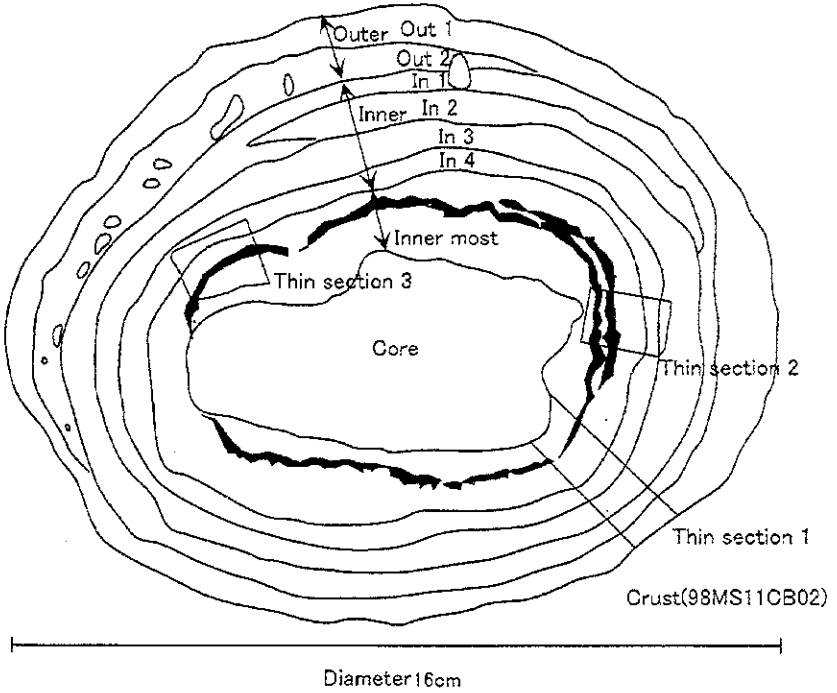

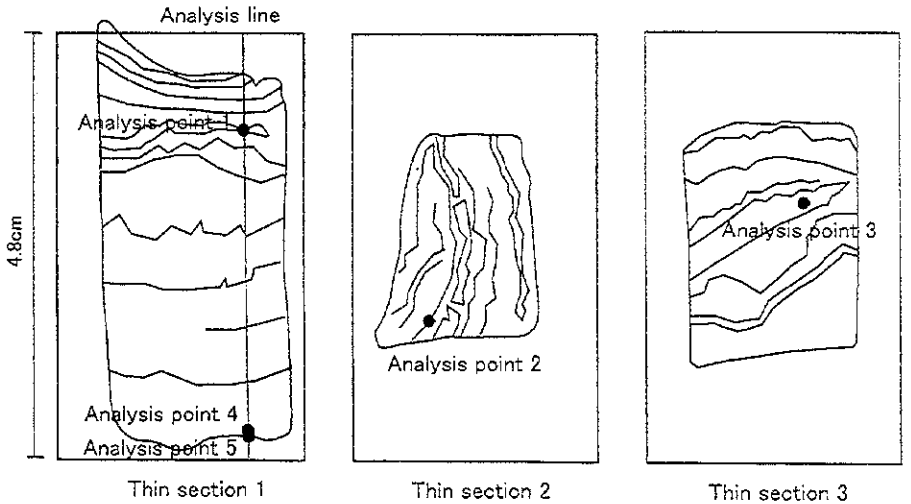

Fig. 5-5-1 Analyzed sample and points of analyses

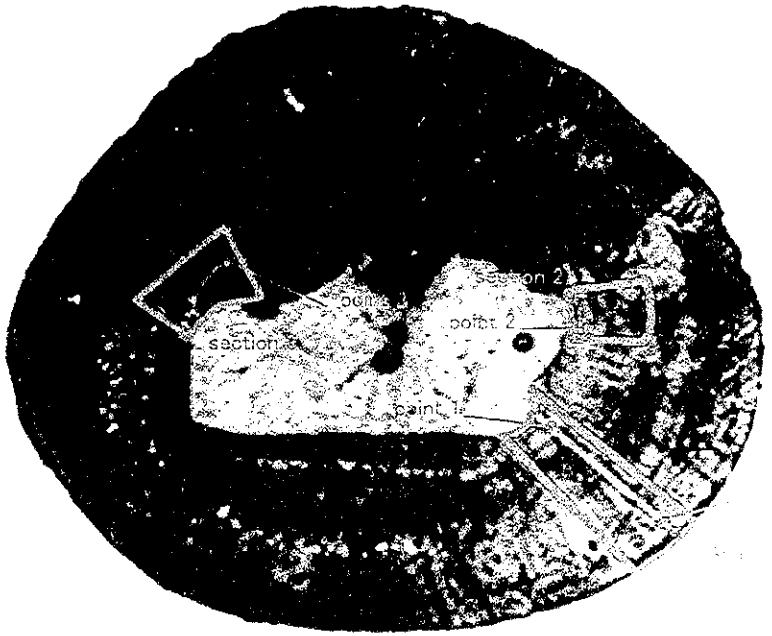

Diameter 18cm

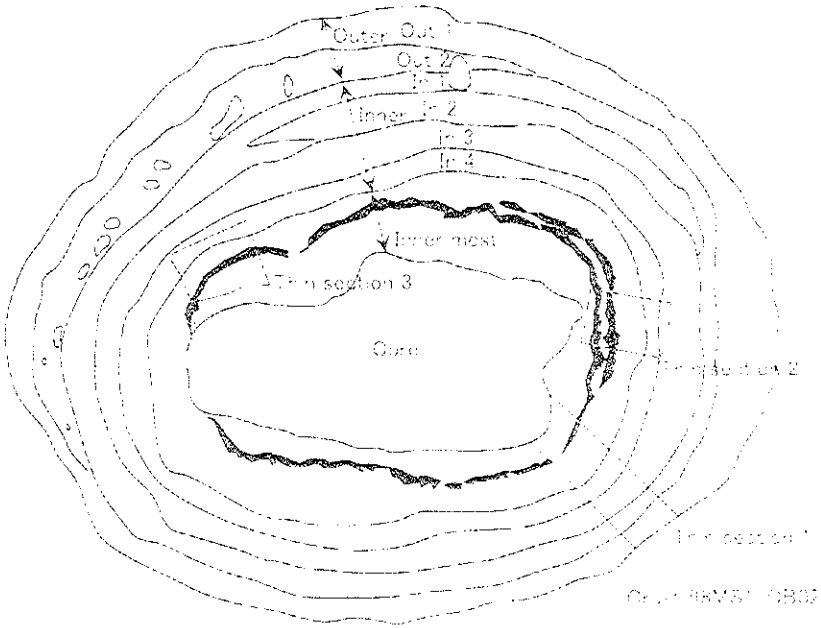

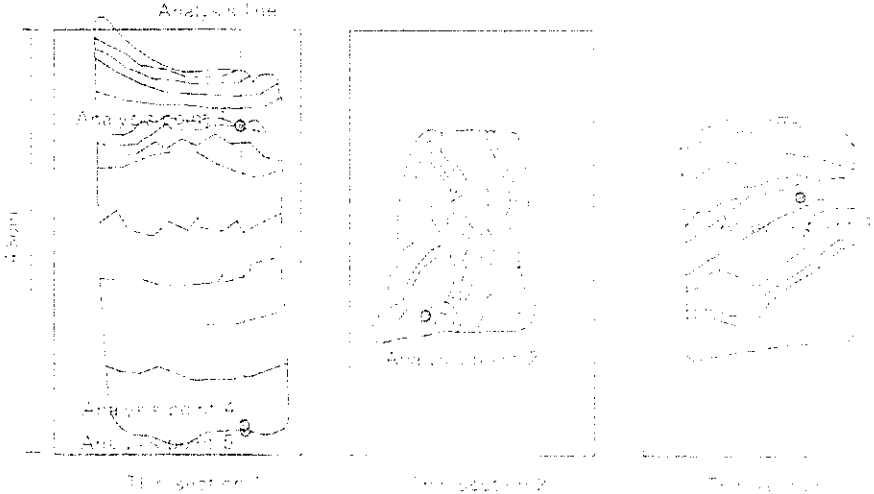

Fig. 5-5-1 Analyzed sample and points of analyses

(3) Interpretation of chemical results

1) Point analysis

The manganese dioxide minerals constituting cobalt-rich crusts are believed to be todorokite, birnessite, buserite, and vernadite. But the marine manganese minerals, with the exception of buserite, do not have definite chemical formula, and are generally minute aggregates of minerals of low cristalinity. Thus mineralogical examination of these minerals is often difficult. It is common to consider them using Mn - Fe - (Cu+Ni+Co)*10 diagram. Therefore, the above results will be discussed on the basis of this triangular diagram.

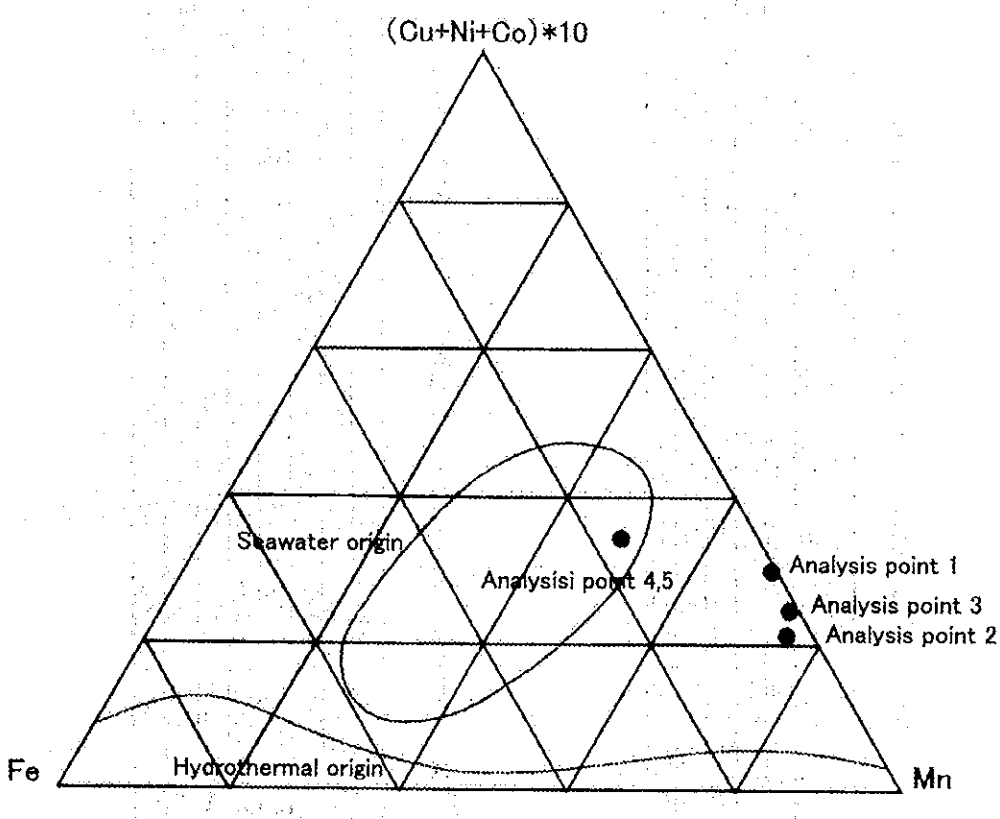

Fig.5-5-2 Mn-Fe-(Cu+Ni+Co)*10 Diagram

Analytical points 1, 2, and 3 are all in the blackish gray layer with metallic luster. The major mineral component of the part in the inner layer is considered to be todorokite from the chemical composition. But all three points are plotted in areas closer to Mn than manganese nodules and cobalt-rich crusts of sea water origin.

Analytical points 4 and 5 are in the black compact part of outer layer 1. The analytical values are similar

Table5-5-3 Results of EPMA point analysis

No.	Thin section	Part	Mn (%)	Co (%)	Fe (%)	Cu (%)	Ni (%)	Pt (%)	P (%)	Si (%)	Na (%)	Mg (%)	Al (%)	S (%)	Cl (%)	Ca (%)	K (%)	Ba (%)	Sr (%)	Mn/Fe	Total (%)
1	1	Inner most	59.50	0.10	0.90	0.51	1.32	<0.10	0.83	<0.10	1.09	2.91	0.88	0.14	0.07	2.16	0.99	7.08	0.31	66.11	78.85
2	2		57.93	0.60	2.42	0.40	0.60	<0.10	0.22	<0.10	1.09	2.28	0.59	<0.10	0.05	1.47	1.03	7.21	0.32	23.94	76.29
3	3		60.33	0.10	0.48	0.38	2.07	<0.10	<0.10	<0.10	1.23	4.93	0.69	<0.10	0.03	0.58	1.95	3.75	0.14	125.69	76.73
4	1	Outer	43.48	1.73	14.04	0.13	1.12	<0.10	0.60	0.51	3.42	2.71	0.52	0.71	1.21	3.86	0.69	0.21	0.10	3.10	75.08
5	1		43.30	1.78	14.08	0.07	1.19	<0.10	0.52	0.44	3.41	2.93	0.47	0.64	1.19	3.71	0.61	0.16	<0.10	3.08	74.60

Table5-5-4 Results of EPMA line analysis

Part	Point No.	Count number								Grade (%)						
		Mn	Co	Fe	Cu	NI	Pt	P	Si	Mn	Co	Fe	Cu	NI	P	Si
First (outer1) Ave.	54	32002	1372	10758	441	566	196	1644	4774	39.42	0.30	2.99	0.28	1.05	1.75	0.41
Third (inner1) Ave.	40	23602	595	12928	453	412	200	8215	7738	28.94	0.12	3.63	0.29	0.75	10.59	0.68
Fifth (inner3) Ave.	57	18293	506	12730	426	268	187	12680	6762	22.32	0.10	3.57	0.27	0.47	16.60	0.59
Sixth (inner4) Ave.	85	22402	640	11978	471	361	195	11746	7450	27.45	0.13	3.35	0.30	0.65	15.34	0.65
Seventh (inner most) Ave.	160	24990	738	10558	445	378	190	10514	5769	30.67	0.15	2.93	0.28	0.68	13.68	0.50
Total	396	24287	755	11442	448	388	193	9649	6336	29.80	0.15	3.19	0.29	0.70	12.52	0.55

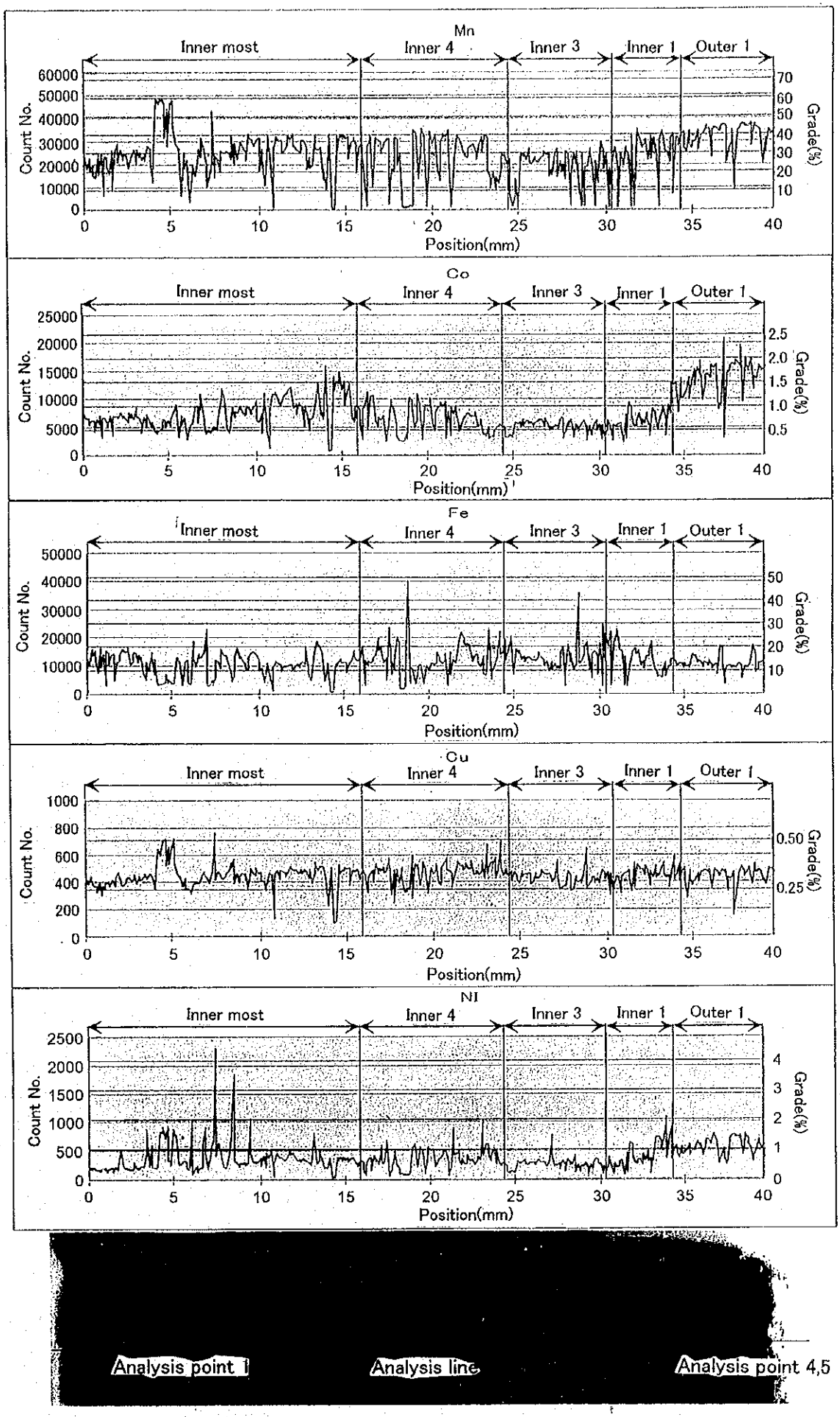

Fig. 5-5-3 Chemical compositional variation

and are plotted in the same point of the triangular diagram. It lies within the area of manganese nodules and crusts of sea water origin of Usui (1996). The Mn grade is 43% for both and is slightly higher than those of other manganese nodules and crusts, and since accessory components Na, Ca contents are not high, the major mineral is inferred to be vernadite.

Line analysis of the inner layer indicate the following.

With the exception of the blackish gray layer, the Mn/Fe ratio is stable at around 2 in the inner layer although there is a peak in some parts. On the other hand, the ratio increases abruptly in the blackish gray layer with a maximum of 14. Also the Cu and Ni grades are clearly different from other parts and show high values. This is believed to be the result of variation of the constituent minerals, and the environment of formation is inferred to have changed at this time.

2) Line analysis

Compositional variation of middle and outer layers confirmed by line analysis is as follows.

Co, Mn, Ni grades are generally slightly low in hard and compact middle layer 4 which contains apatite, while the Fe, P grades are high. This is considered to be caused by the mixture of apatite. Co grade tends to gradually decrease outward. The Fe grade varies notably by measuring points.

Compact, hard, and iron oxide-bearing middle layer 3 has generally low Mn, Ni, Co, Cu grades while Fe, P, Si grades are high. Generally Mn, Fe, Cu grades gradually decrease outward.

Metal grades of apatite-bearing middle layer 1 have tendency similar to middle layer 4 which also contain apatite for six elements with the exception of Ni. Mn, Co, Ni grades tend to gradually increase outward and this trend continues to outer layer 1. Ni grade decrease slightly near the boundary with outer layer 1.

Compact and hard outer layer 1 has generally high Mn, Co, Ni grades. P grade is low and Fe grade also is slightly low. Co grade gradually increase outward, and it is the highest of this ore at the outerside.

Regarding the whole ore, if the effect of apatite and quartz is eliminated, Co, Ni grades tend to increase outward. Mn grade also tends to increase outward, but in some cases, such as middle layer 3, it tends to decreases. The content of Fe is strongly influenced by impurities such as apatite. Cu does not have any set tendency regarding it content.

5-6 Conditions of Cobalt-rich Crust Occurrence

The area surveyed during 1996 and the present project comprises approximately the northwestern half of the EEZ of the Republic of Marshall Islands, and the distribution of seamounts and the conditions of cobalt-rich crust occurrence in the area are as follows.

Pointed seamount was surveyed in only one easternmost area in 1996, and it is characterized by relatively high cobalt grade but young age (35Ma).

Most of the seamounts in the surveyed 13 areas are guyots and their summit topography is further divided into; six dome-shaped, four flat, and two rugged seamounts. Area-wise, the flat and rugged summit seamounts occur at the eastern and western end of the area and the dome seamounts in the central part of the survey area. The unconsolidated sediments on the summit seen as the SBP transparent layers tend to be thin on flat summit and thick on dome-shaped ones.

The results of sampling and seafloor observation show that crusts thicker than 10cm occur at 1,000~3,500m water depth. Cobalt-rich crusts take the forms of; crusts, cobble crusts, and nodules. Their thickness varies by areas, topography, and substrates. The average thickness of the crusts by seamounts tends to be thicker to the west and the metal grade higher to the east. This tendency, however, is observed but is not clear- cut.

In assessing the potential of each area by the occurrence of the crusts; the seamounts in the western part of the area surveyed this year are most promising, followed by the seamounts continuing to the northern part of the Ralik Chain. This is due to the thick crusts in the western side and the high grade in the eastern side.

The mode of occurrence of cobalt-rich crusts in areas surveyed this year is summarized in Table 5-6-1.

Table 5-6-1 Characteristic of occurrence of cobalt-rich crust

Area	Scale of seamount	Topographic of seamount			Crust exposure		Crust thickness(mm)		Average		
		Roughness	Gradient of flank	Depth of summit	Summit	Flank	maximum	Average	Co(%)	Ni(%)	Pt(ppm)
MS10	small	a little	17°	1,292m	low	high	115	44.0	0.69	0.47	0.67
MS11	moderate	moderate	11°	1,495m	low	moderate	140	38.6	0.69	0.48	0.61
MS12	small	a little	17°	1,037m	moderate	high	140	33.1	0.67	0.56	0.47
MS13	big	much	7°	1,387m	low	low	160	46.4	0.50	0.39	0.37

The undulations of the seamounts are based on seafloor topographic map and the degree of crust exposure is based on MBES acoustic pressure map. The crust thickness and the grade are based on the actual measured values.

The crusts from the seamount in MS11 have high Co, Cu, grades and MS12 area has high Ni, Mn grade. But metal grades of the seamounts in three areas of MS10~MS12 are comparable and not much different, while the seamount in MS13 area has lower Co, Ni, Cu grades than the other three areas.

The crusts are thinnest in MS12 area, but crust exposures occur widely from the summit periphery to the middle slope, and thick crusts occur throughout the seamount.

The crusts are exposed widely on the upper slope of the seamount in MS10 area. But the thick crusts are concentrated to relatively near the periphery and the seamount is small. Thus the exposed area of thick crusts is believed to be relatively small.

The average thickness of the crusts is 38mm in MS11 area, but crust exposure is restricted to the summit periphery, parts of the slope, and at the summit pinnacles. The size of the seamount, however, is relatively large and, as a whole, thick crusts occupy a large area.

MS13 area provided the thickest crust sample in this survey area, and the average thickness is large. It is highly possible that thick crusts occur over the whole seamount, but this year, thick crusts could be confirmed only in limited area near the pinnacles.

The four seamounts surveyed this year are all promising with thick crust distribution, but further integrated assessment shows that MS11 and MS12 areas would be most promising followed by MS10 area. But the difference among the three areas is small. MS13 area is evaluated as lower than the other three areas, MS10~MS12, in terms of metal grade.